Ergosterol reduction impairs mitochondrial DNA maintenance in S. cerevisiae

"Ergosterol reduction impairs mitochondrial DNA maintenance in *S. cerevisiae*"

Angela Cirigliano[*], Alberto Macone[‡§], Michele Maria Bianchi[*], Simonetta Oliaro-Bosso#, Gianni Balliano#, Rodolfo Negri[*°] and Teresa Rinaldi[*§‖]

[*] Department of Biology and Biotechnology "Charles Darwin", La Sapienza University of Rome, Piazzale A. Moro 5, 00185 Rome, Italy.

[§]Pasteur Institute-Cenci Bolognetti Foundation, Viale Regina Elena, 291, 00100 Rome, Italy.

° Institute of Molecular Biology and Pathology, CNR, Department of Biology and Biotechnology "Charles Darwin", La Sapienza University of Rome, Piazzale A. Moro 5, 00185 Rome, Italy.

[‡] Institute of Molecular Biology and Pathology, CNR, Dipartimento di Scienze Biochimiche "A. Rossi Fanelli", La Sapienza University of Rome, Piazzale A. Moro 5, 00185 Rome, Italy.

#Dipartimento di Scienza e Tecnologia del Farmaco, University of Turin Via Pietro Giuria 9 - 10125 Torino, Italy.

[‖]Corresponding author. Address: Piazzale A. Moro 5, 00185 Rome, Italy; Tel: +39-06-49912259; e-mail: teresa.rinaldi@uniroma1.it

Abstract

Sterols are essential lipids, involved in many biological processes. In *Saccharomyces cerevisiae*, the enzymes of the ergosterol biosynthetic pathway (Erg proteins) are localised in different cellular compartments. With the aim of studying organelle interactions, we discovered that Erg27p resides mainly in Lipid Droplets (LDs) in respiratory competent cells, while in absence of respiration, is found mostly in the ER. The results presented in this paper demonstrate an interplay between the mitochondrial respiration and ergosterol production: on the one hand, rho° cells show lower ergosterol content when compared with wild type respiratory competent cells, on the other hand, the ergosterol biosynthetic pathway influences the mitochondrial status, since treatment with ketoconazole, which blocks the ergosterol pathway, or the absence of the *ERG27* gene, induced rho° production in *S. cerevisiae.* The loss of mitochondrial DNA in the Δ*erg27* strain is fully suppressed by exogenous addition of ergosterol. These data suggest the notion that ergosterol is essential for maintaining the mitochondrial DNA attached to the inner mitochondrial membrane.

Keywords: ergosterol, mitochondria, rho° cells, *S. cerevisiae*, lipid droplets, sterols.

Abbreviation: ER, Endoplasmic Reticulum; LDs, Lipid Droplets; mt, mitochondria; wt, wild type.

1. Introduction

Sterols are essential lipid components which control fluidity and permeability of membranes [1]. The cholesterol content is tightly regulated, minor changes in its amount has an impact on cellular functions [2]. In mammalian cells, cholesterol is the principal sterol, also used as a precursor of steroids and bile acids. Disorders in cholesterol metabolism lead to human diseases, including neurodegeneration [3, 4].

The yeast *S. cerevisiae* synthesizes ergosterol through a complex pathway of more than twenty reactions [5-7] catalysed by enzymes (Erg proteins) located in different cellular compartments: cytoplasm, endoplasmic reticulum (ER) and Lipid Droplets (LDs) (Figure 1). The ergosterol biosynthetic pathway is conserved in evolution and seventeen out of nineteen tested genes were replaceable by the human counterpart [8].

In *S. cerevisiae*, ergosterol is an essential component of all cellular membranes, including organelle membranes. The mitochondrial concentration of ergosterol is different between the inner mitochondrial membrane (IMM) and in outer mitochondrial membrane (OMM). Of note, the IMM is more enriched in ergosterol than the OMM (6μg ergosterol per mg of organellar protein in the outer membrane and 25μg/mg in the inner membrane) [9, 10]. Ergosterol is actively transported into the OMM in an energy independent way [11, 12]. Mitochondria have an essential role in lipid metabolism and communicate with other organelles such as Endoplasmic Reticulum (ER), Lipid Droplets (LDs) and peroxisomes [13-17]. In yeast, the ER–Mitochondrial Encounter Structure (ERMES) complex (Mdm34p, Mmm1p, Mdm12p and Mdm10p) tethers ER and mitochondria. This complex is an important " hub" because the ER-mitochondria contact sites are involved in phospholipid exchange, mitochondrial division, distribution and morphology and maintenance of mitochondrial DNA [18, 19]. This complex is not conserved in metazoan but its essential functions are assured by different complexes and recently the human homologue of Mmm1p has been identified [20-24]. While phospholipid biogenesis has been extensively investigated at the contact site between ER and mitochondria, less is known about ergosterol function in yeast mitochondria [25, 26]. It is also unclear whether ergosterol transport to mitochondria is facilitated by direct membrane contacts, either between ER and mitochondria or between Lipid Droplets and mitochondria [11]. It has been observed that yeast cells lacking the ERMES complex have altered level of ergosterol, pointing to a role of the ER-mitochondrial contact site for sterol exchange [27]. Indeed, *ERG24*, *ERG28* and *ERG6* genes were isolated in a screening for

mutants defective in mitochondrial distribution and morphology [28] and mitochondrial morphogenesis and inheritance rely on the presence of the ergosterol biosynthetic enzymes since transcriptional down regulation of the ergosterol genes results in mitochondrial membrane alteration [29].

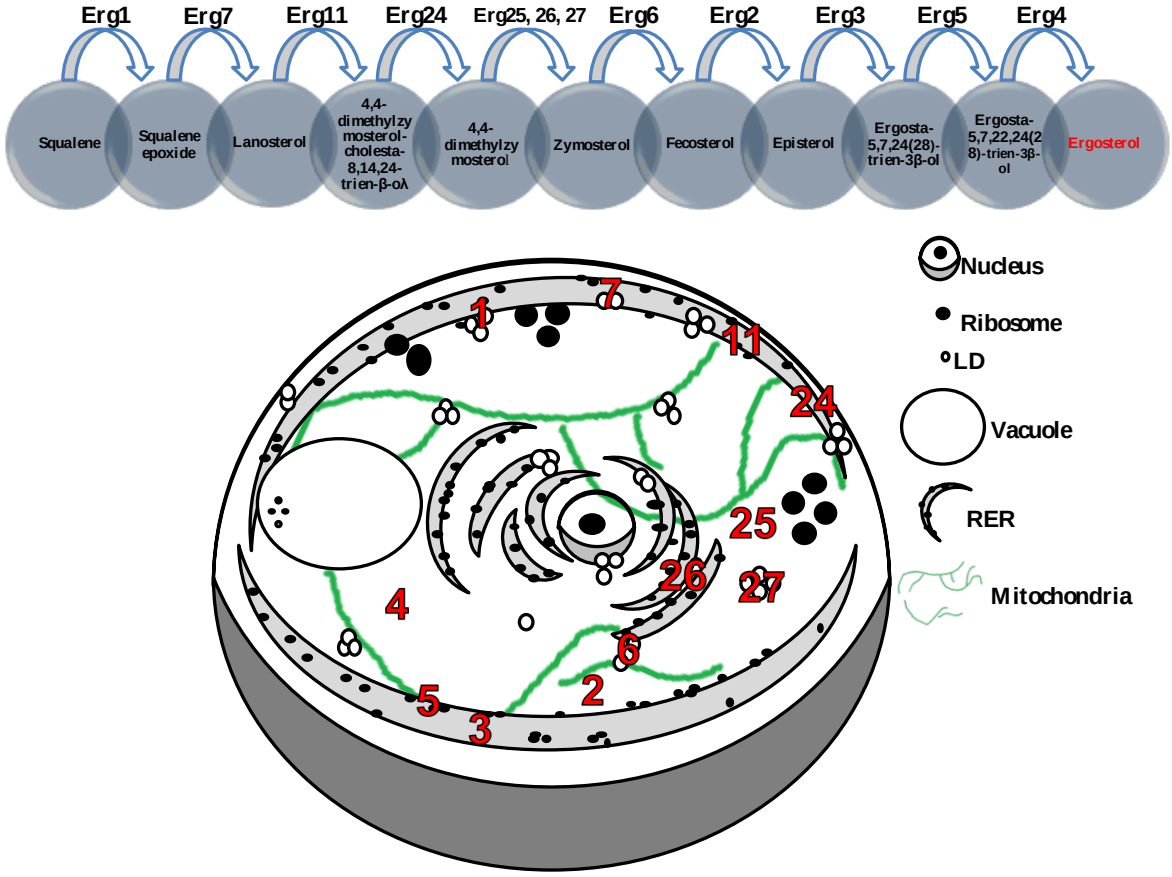

Figure 1. Localisation of the yeast ergosterol biosynthetic pathway enzymes (*ERG*) in cytoplasm, Endoplasmic Reticulum (ER) and Lipid Droplets (LDs). The enzymes of this pathway are essential for life till Erg25p-26p-27p complex.

We sought to investigate the relationship between mitochondria and LDs and we discovered that, on the one hand, in yeast cells lacking mitochondrial DNA or with a block of respiration (dysfunctional mitochondria), the Erg27p enzyme moves from LDs to ER and the ergosterol content is low in these cells; on the other hand, the block of the ergosterol biosynthetic pathway with ketoconazole leads to the loss of mitochondrial DNA (rho° cells), and the yeast strain deleted for *ERG27* gene shows high *petites* production (cells devoid of mitochondrial DNA), a phenotype which is suppressed by adding ergosterol in the medium culture. These results suggest a cross talk between mitochondria and the ergosterol biosynthetic pathway, demonstrating the essential function of ergosterol in the maintenance of mitochondrial DNA in yeast cells.

2. Material and Methods

2.1 Yeast strains and growth conditions

The strains used in this study were derived from W303 *(MAT a, his3-11, ade2-1, leu2-3, -112, ura3-1, trp1-1, can1-100)* or BY4741 genetic context *(MAT a, his3Δ1, leu2Δ0, met15Δ0, ura3Δ0)*. The strains used in this study were generated by mating, sporulation and tetrad dissection. The Δ*erg27* genotype is: *MATa, upc2-1, hap1Ty, ura3, his3, leu2, trp1, erg27Δ::LEU2*; the Δ*mdm34* genotype is *MAT a, his3-11, ade2-1, leu2-3,-112, ura3-1, trp1-1, can1-100, mdm34Δ::URA3.* The Δ*rtg2* genotype is: *MAT α, his3-11, ade2-1, leu2-3, -112, ura3-1, trp1-1, can1-100, rtg2Δ::LEU2.* To verify the percentage of *petites* production of a strain containing only the *upc2-1* mutation, we used the Δ*erg27* strain transformed with a plasmid expressing the wild type *ERG27* gene (pST10(ERG27)) [30]. The plasmid pVT100U-mitoGFP was used to visualize mitochondria [31].

Yeast culture media: YPD (1% bacto peptone, 1% yeast extract and 2% glucose), was used as rich medium. YPG (1% bacto peptone, 1% yeast extract and 3% glycerol), was the medium used to verify the respiratory competence of yeast colonies. W0 (0.17% yeast nitrogen base, 0.5% ammonium sulphate and 2% glucose) was used as minimal medium. All media were supplemented with 2.3% bacto agar (Difco) for solid media and W0 was supplemented with the appropriate nucleotides requirements according to the phenotype of the strains. The Δ*erg27* strain is grown in YPD medium supplemented with 0.02mg/ml of ergosterol. Ergosterol and Tween 80 were dissolved in pure ethanol to final concentration of 10 mg/ml for ergosterol and 42% for Tween 80, and steamed at 100°C for 10 minutes, always protected from light, before being added to the medium [32, 33].

Yeast cultures were grown and analyzed in exponential phase at 28°C, unless otherwise specified.

2.2 Rho° production

Strains (W303 or BY4741 genetic context) devoid of mitochondrial DNA were produced as follows: cells were grown at the density of $1x10^6$cells/ml on YPD medium, phosphate buffer pH 6.5 was added in 1 ml of culture, at the final concentration of 0.05M, and ethidium bromide at final concentration of 50 μg/ml. The cultures were incubated at 28°C for 24h. Cells were washed twice, plated on YPD and incubated at 28°C.

The absence of mitochondrial DNA was assessed by DAPI staining and absence of growth on glycerol containing medium as a carbon source.

2.3 *Petites* assay

Cells were grown in YPD (supplemented with 0.02mg/ml ergosterol for the Δ*erg27*) until the stationary phase. From these cultures, cells were inoculated in YPD supplemented with 0.02mg/ml ergosterol. At the concentration of $1x10^7$cells/ml and $1x10^8$cells/ml, 100 cells were spotted in YPD plates and incubated at 28°C. After two days, colonies were replicated on YPG plates. Cells grew only on YPD and not on YPG plates are *petites*, DAPI staining was performed to verify the complete absence of mtDNA (rho° cells).

2.4 Microscopy

Cells were observed with a Zeiss Axio Imager Z1 Fluorescence Microscope with AxioVision 4.8 Digital Image Processing System, the objective lens used was 63x Oil (Figure 2, 3, 7, 9 and Supplemental Figure 1) [34]. Filter sets: 38HE (GFP), 43HE (DsRed). Filters for GFP (470/40 nm excitation and 525/50 nm emission), and RFP (550/25 nm excitation and 605/70 nm emission) were used. Better selectivity for cytoplasmic Lipid Droplets was obtained when the cells were viewed for yellow-gold fluorescence (excitation, 450-500 nm; emission, greater than 528 nm) rather than red fluorescence (excitation, 515-560 nm; emission, greater than 590 nm): for this reason, Nile Red was observed with GFP filter [35]. Metamorph software (Universal Imaging, West Chester, PA) was used to deconvolute Z-series and treat the images.

2.5 Nystatin and Ketoconazole assay

Cells were grown to a density of $1x10^7$ cells /ml in YPD rich medium supplemented with different Nystatin and Ketoconazole (Sigma Aldrich) concentration and a total of 100 cells were plated on YPD plates incubated at 28°C for two days [36]. Colonies were counted and counts plotted into a graph.

2.6 Mass spectrometric analysis

Dry cell pellets were deep frozen by immersion in liquid nitrogen and quickly ground to a powder using an IKA A11 basic laboratory mill (IKA, Staufen, Germany). 300 mg of cell pellet were transferred to glass vials with 10ml Folch solvent (chloroform/methanol 2:1, v/v) containing 0.01% butylated hydroxytoluene followed by the addition of 10 µl of internal standard (19-hydroxy-cholesterol, 2 mg/ml in methanol) as internal standards (IS). The homogenization and extraction (60 min) were carried out at room temperature (RT). The extracts were evaporated under a stream of N_2 then the dry residue was dissolved in 1ml hydrolysis solution

containing 5% KOH in (MeOH/H_2O, 95:5) and subjected to saponification (1h, 80°C). The hydrolysed solution was extracted with 0.5ml distilled H_2O and 4ml diethyl ether. The ether phase was dried under a stream of N_2 at RT. The samples were then reconstituted with 25µl ethylacetate and vortex mixed. The fractions to be analysed were converted to their trimethyl-silylated derivatives by heating with 40µl BSTFA containing 1% TMCS at 70°C for 45 min. The sample was dried under a stream of N_2. The residue was dissolved in 200ml hexane and the clear hexane phase was transferred into a glass vial for GC–MS injection. GC-MS analyses were performed with an Agilent 6850A gas chromatograph coupled to a 5973N quadrupole mass selective detector (Agilent Technologies, Palo Alto, CA, USA). Chromatographic separations were carried out with an Agilent HP5ms fused-silica capillary column (30m × 0.25mm i.d.) coated with 5%- phenyl-95%-dimethylpolysiloxane (film thickness 0.25µm) as stationary phase. Injection mode: splitless at a temperature of 280°C. Column temperature program: 120°C (1min) then to 320°C at a rate of 5°C/min and held for 5 min. The carrier gas was helium at a constant flow of 1.0ml/min. The spectra were obtained in the electron impact mode at 70eV ionization energy; ion source 280°C; ion source vacuum 10-5Torr. MS analysis was performed simultaneously in TIC (mass range scan from m/z 50 to 800 at a rate of 0.42 scans s-1) and SIM mode. For GC-SIM-MS analysis, ion m/z 363 was selected for ergosterol and ion m/z 353 was selected for the internal standard.

2.7 Real Time RT-PCR

1 µg of total RNA extracted from cell cultures was reverse transcribed using 200ng of 16mers oligo dT (Life technologies) with SuperScript III First-Strand Synthesis System for RT-PCR (Life technologies), according to the manufacturer's instructions. cDNA served as template for subsequent Real Time PCR reactions that were set up in duplicate for each sample using the SensiMix SYBR Mix (Bioline, London, United Kingdom) and an Applied Biosystems Prism 7300 Sequence Detector. The reaction mixtures were kept at 95°C for 10 min, followed by 40 cycles at 95°C for 15 sec and 60°C for 1 min. The threshold cycle (Ct) was calculated using the Sequence Detector Systems version 1.2.2 (Life technologies) by determining the cycle number at which the change in the fluorescence of the reporter dye (ΔRn) crossed the threshold. To synchronize each experiment, the baseline was set automatically by the software. Relative quantification was carried out with the $2^{-\Delta\Delta Ct}$ method, using the abundance of Actin transcript as endogenous house-keeping control. Data were statistically analyzed by Student's t-test.

2.8 Western blot

10 ml of cells grown to 1×10^7 cell/ml are extracted by performing trichloroacedic acid (TCA) protein precipitation. Proteins are resolved on 10% Tris–glycine PAGE, transferred to PVDF membranes and immunoblotted using the a-Gfpp antibody (Santa Cruz Biotechnology, Santa Cruz, CA) and a-Ada2p antibody (Santa Cruz Biotechnology, Santa Cruz, CA). The secondary antibody was anti-Goat (Santa Cruz Biotechnology) and anti-Rabbit (Santa Cruz Biotechnology). The proteins were visualized utilizing the Bio Rad's ChemiDoc XRS+system, according to manufacturer's instructions. Erg27p-GFP bands were quantified with Image Lab 5.1 version software by Bio Rad.

2.9 Incorporation of [^{14}C] acetate into non-saponifiable lipids of yeast cells

Sterol biosynthesis in whole yeast cells was followed by incorporation of [^{14}C] acetate into non-saponifiable lipids as described previously [30]. Briefly, washed cells (1×10^8 cells) were resuspended in 1ml of fresh media, incubated with 0.1 μCi of [^{14}C]acetate ([1,2-^{14}C]acetate (50 μCi, 1.85 MBq) from Perkin-Elmer, Italy) in presence of Tween-80 (0.2 mg/ml) and shaken for 3 h at 30°C. Cells were then saponified in 1ml of methanolic KOH (15% w/v) for 30 min at 80°C. Non-saponifiable lipids were extracted with petroleum ether and separated on TLC plates (20×20 cm×0.25 mm) using cyclohexane/ethyl acetate (85:15; v/v). Squalene, oxidosqualene, dioxidosqualene, lanosterol, ketosteroid 1 (a mixture of 4-methylzymosterone and 4-methylfecosterone), ketosteroid 2 (a mixture of zymosterone and episterone) and ergosterol were used as references. Radioactivity in separated bands was measured by collecting counts over a 5 min period with a System 200 Imaging Scanner (Hewlett- Packard, Palo Alto, CA, USA).

2.10 Vitality - Standard Plate Count (SPC)

Cells were grown in exponential phase in YPD rich medium supplemented with nystatin or ketoconazole (Sigma Aldrich). After 24 hours cells were counted with the Bürker chamber and diluted with sterile deionized water to spread 100 cells in each YPD plate (five independent experiments). The plates were incubated at 28°C for 48 hours and individual colonies we counted to calculate the percentage of viability [37]. The same experiment was performed at 48, 72, and 96 hours.

3. Results

3.1 Erg27p mostly resides in ER in rho° cells

An interactomic study between LDs and mitochondria showed that Erg6p (LDs resident protein) physically interacts with mitochondrial outer membrane proteins [38]. We were interested to investigate LDs-mitochondrial interactions in a ERMES defective strain; to this purpose, we used a strain deleted for the *MDM34* gene containing the *ERG27-GFP* fusion in the *ERG27* locus, to visualize the localization of the protein by fluorescence microscopy (see Materials and Methods). We chose to investigate the Erg27p because it is essential and mainly LD localized. The Erg27p fused to *GFP* is fully functional [39]. As a control, we used a W303-*ERG27-GFP* devoid of mitochondrial DNA (rho°) because Δ*mdm34* (previously named Δ*mmm2*) is a rho° respiratory impaired strain [40]; the reason why Δ*mdm34* is devoid of mitochondrial DNA is because this protein is part of the ERMES complex, crucial in coordinating mitochondrial DNA division and replication [41, 42]. As expected, in a wild-type strain Erg27p-GFP was mainly located in LDs [43]. Surprisingly, in Δ*mdm34* and in wild-type rho° strain, used as a control, the Erg27p-GFP mainly decorated nuclear and cortical ER, Figure 2A (we obtained the same result also with strains deleted for the other ERMES subunits, not shown). Since Erg2p-GFP is localized in the ER also in the wild-type rho° control strain, the Erg27p delocalization was presumably not due to the absence of a functional ERMES complex itself, but rather to the lack of mtDNA. We then decided to investigate if the Erg27p localization in nuclear and cortical ER in rho° cells could have a physiological significance. It was previously observed that in a yeast mutant devoid of LDs, some enzymes of the ergosterol biosynthesis, usually positioned in LDs, were retained in the ER [44]. We therefore tested the presence of LDs in W303 and W303 rho° cells by using Nile Red staining. Figure 2B shows that the LDs were present, indicating that the ER location of Erg27p in a rho° strain was not due to a major alteration of LDs biogenesis; of note, we observed a lower amount of LDs in W303 rho° and in Δ*mdm34*. Figure 2C shows the percentage of cells in which Erg27p is exclusively present in LDs or in ER or in LDs and in ER in the same cell.

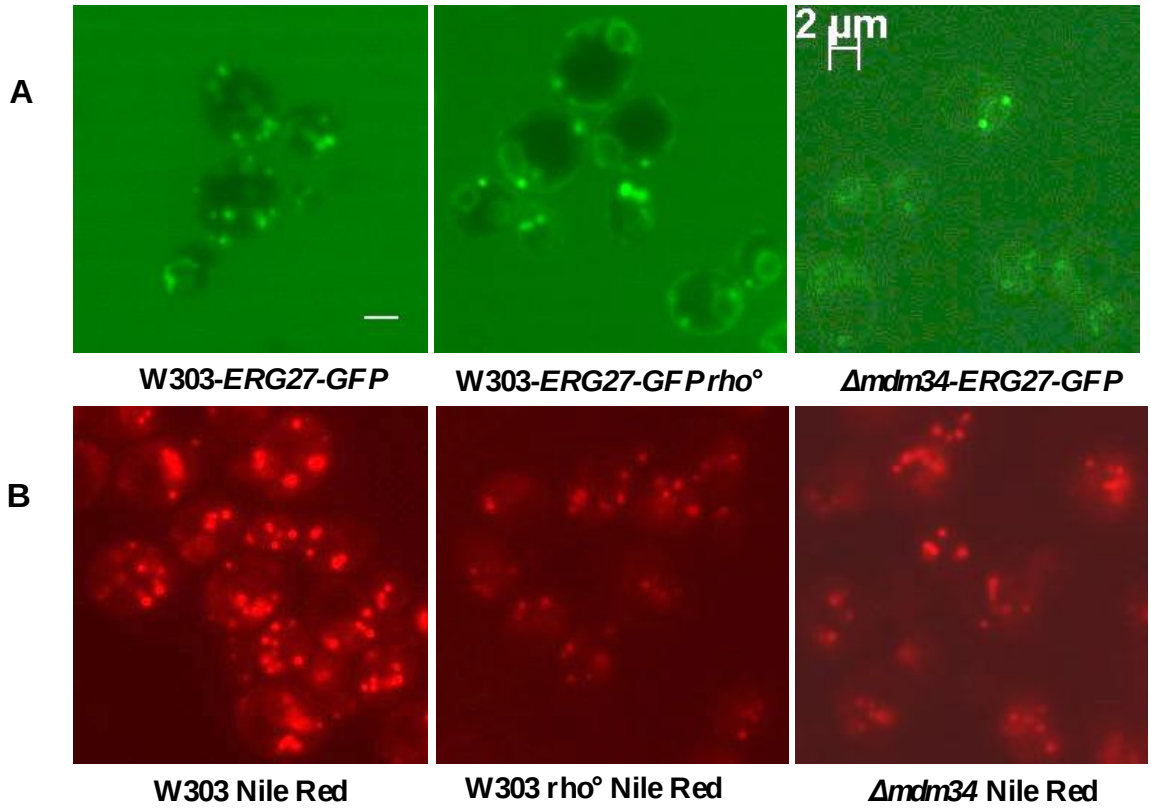
A
2 µm
W303-ERG27-GFP
W303-ERG27-GFP rho°
Δmdm34-ERG27-GFP
B
W303 Nile Red
W303 rho° Nile Red
Δmdm34 Nile Red

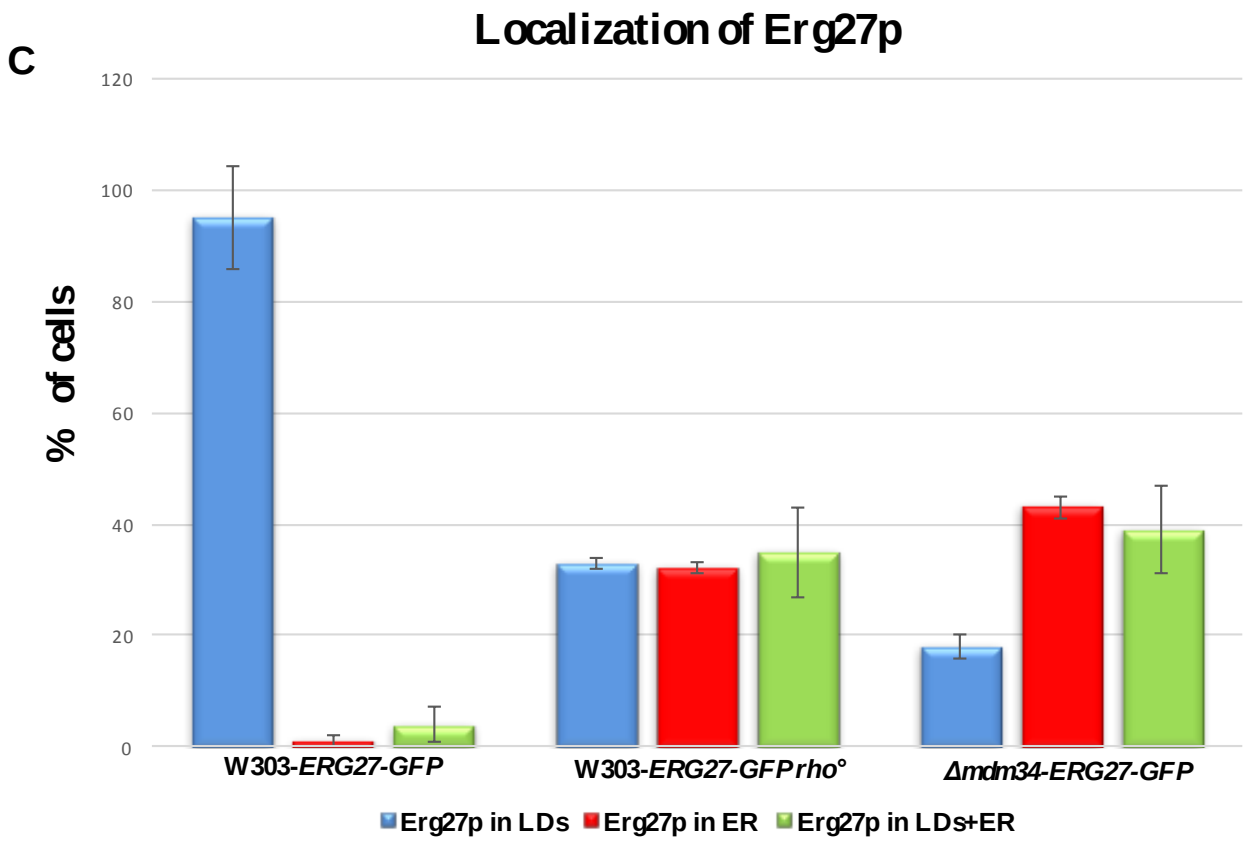
C
Localization of Erg27p
% of cells
120
100
80
60
40
20
0
W303-ERG27-GFP
W303-ERG27-GFP rho°
Δmdm34-ERG27-GFP
Erg27p in LDs
Erg27p in ER
Erg27p in LDs+ER

Figure 2. The Erg27-GFP protein is mainly ER localised in strains devoid of mtDNA (rho° cells). (A) Erg27p-GFP localization in W303, W303 rho° and Δ*mdm34* strains in exponential growth phase in YPD. (B) Lipid Droplets visualization with Nile Red. Bar: 2μm. The magnification is the same in each picture of Figure 2. (C) Quantitative analysis of Erg27-GFPp localization. Erg27p in LDs means that Erg27p is visualized in a cell only in LDs. Erg27p in ER means that Erg27p is visualized in a cell only in ER, and Erg27p in LDs+ER means that Erg27p is visualized in a cell both in LDs and ER. (Data are the average of four independent experiments and standard deviation is indicated).

3.2 Transfer of Erg27p from LDs to ER after treatment with antimycin A

To explore the dynamics of Erg27p localization in cell compartments still containing mitochondrial DNA but with an impairment of mitochondrial function, W303 wild-type cells were treated with antimycin A. This drug rapidly acts on yeast cells blocking the cytochrome c reductase on the respiratory chain [45]; Erg27p-GFP was visualized by microscopy from t=0 till 1 hour after addition of 10 μg/ml (final concentration) of antimycin A. At 3 minutes from antimycin addition, Erg27p-GFP was found to have moved in the ER (Figure 3A). As a control, we visualized Erg6p, which is mainly located in LDs; after 10 minutes, in the wild type strain W303-*ERG6-RFP* treated with antimycin A, Erg6p was not relocalized (Figure 3B).

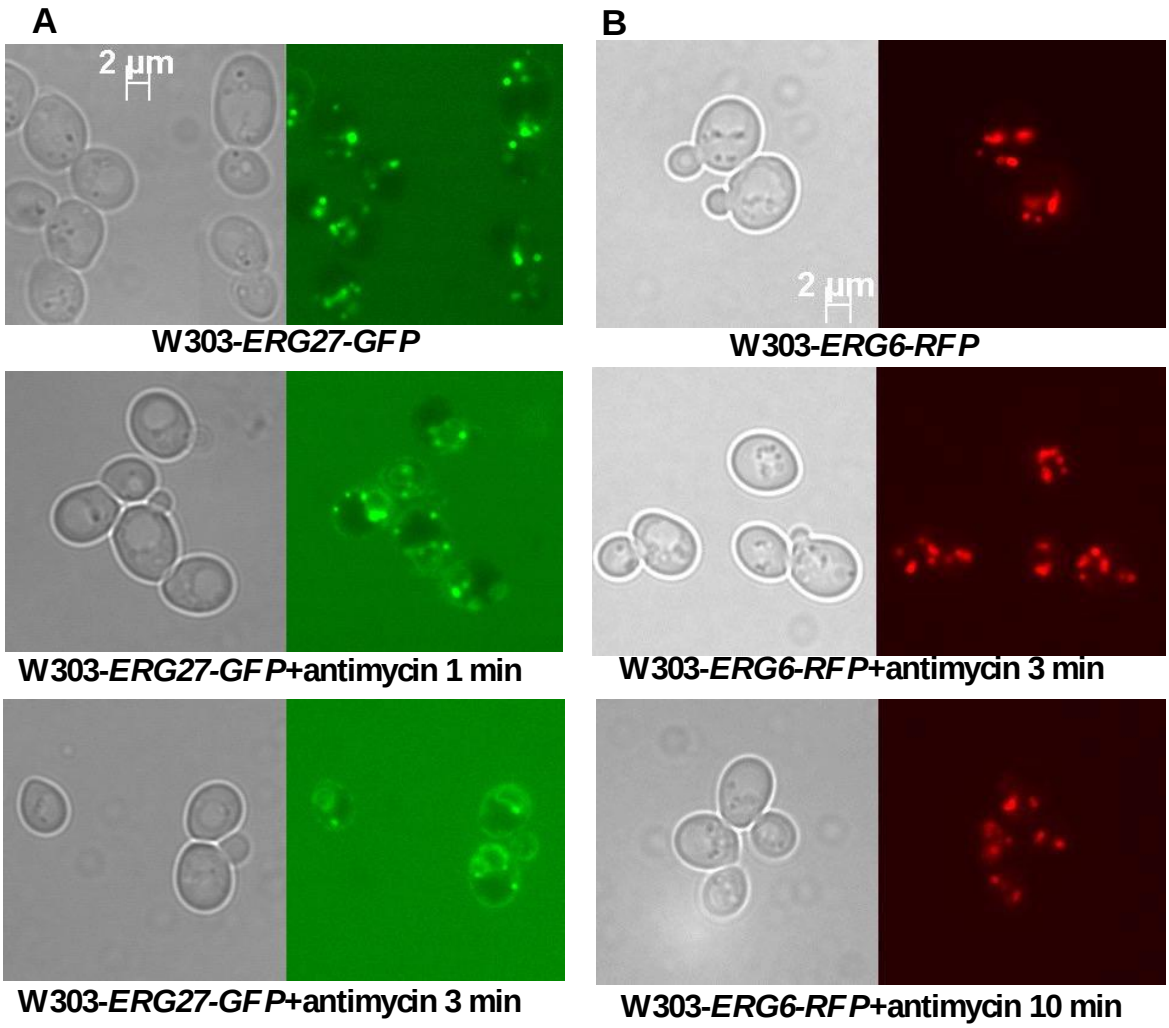

Figure 3. Antimycin A induces a Erg27p relocalization from LDs to ER. (A): in wild type W303 cells treated with antimycin (10µg/ml), Erg27p-GFP relocalized in nuclear and cortical ER in 3 minutes. (B): Erg6p-RFP a LDs resident enzyme, is correctly localized in LDs wild type strain after antimycin treatment. Bar: 2µm. The magnification is the same in each picture.

We observed the cells till one hour after the treatment and, while Erg27p was still located at the ER, Erg6p was still visible in LDs (data not shown). These experiments indicated that the block of the respiratory chain and localization of Erg27p in the ER were strongly correlated and that relocalization was not due to an indirect effect in rho° cells.

To verify the specificity of ER positioning of Erg27p in rho° cells, we investigated the location of Erg7p, using a rho° *ERG7-GFP* strain (Supplemental Figure 1); this enzyme of the ergosterol biosynthetic pathway is transported or escorted in LDs by Erg27p, which performs a chaperon function in addition to the reductase activity [46]. Indeed, in yeast, sterol biosynthesis the 3-keto reductase protein (Erg27p) is required for

oxidosqualene cyclase (Erg7p) activity [47-48]. In absence of mitochondrial DNA, the Erg7p enzyme is correctly associated with LDs and not delocalized.

The relocalization of Erg27p in ER, following a block of mitochondrial function, is specific, since the other two enzymes, mainly found in LDs (Erg6p and Erg7p), are not moved to ER.

3.3 Ergosterol content is lower in rho° cells compared with the isogenic wild-type strain

To investigate if the Erg27p location in ER could alter the biosynthetic ergosterol pathway, we measured the ergosterol content in a wild type and a rho° strains by gas chromatography-mass spectrometry. The quantification was performed in W303, the W303 rho° strain and in Δ*mdm34* (rho° cells). Results reported in Figure 4 revealed that in rho° cells the ergosterol content was significantly lower compared with the wild type isogenic strain. We did not investigate further Δ*mdm34* strain or ERMES as responsible of the Erg27p delocalization because the alteration of the ergosterol content was due to the lack of mtDNA/lack of respiration and not primarily to the absence of ERMES function.

This finding suggests that, in absence of functional mitochondria, the biosynthetic ergosterol pathway is altered resulting in lower ergosterol content in the cells.

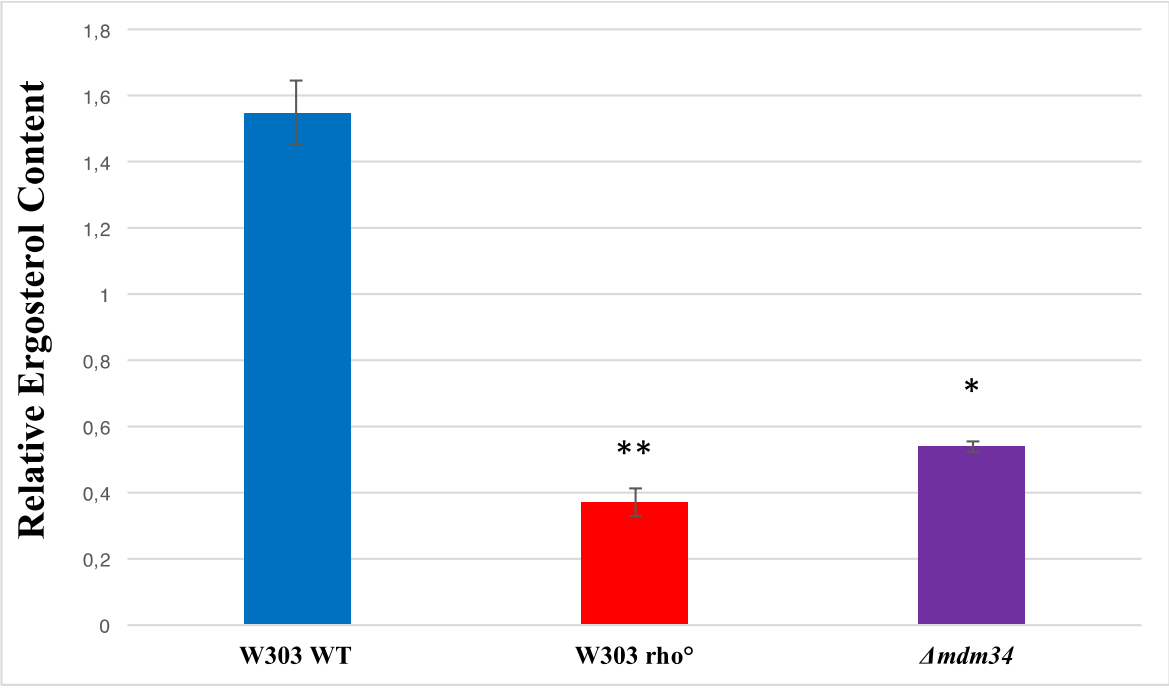

Figure 4. Ergosterol is in lower amount in the rho° strain and in Δ*mdm34*, if compared with wild-type isogenic strain. Gas chromatography-mass spectrometry analysis was performed to measure the ergosterol area/internal standard area. Data are the average of 3 independent experiments and standard deviation is indicated. The asterisks indicate significant modulation (* $p<0.05$) (** $p<0.01$) according to Student's T-test.

3.4 Erg27p maintained its functionality when it is relocalized in ER

To verify if the relocalization of Erg27p in ER occurring in rho° cells impair the functionality of the enzyme, pulse labeling experiments were performed. These experiments are designed to determine the relative amounts of post-squalene intermediates of ergosterol biosynthesis, not the absolute amount/content of ergosterol in the cells. Wild type and rho° cells in two different genetic contexts (W303 and BY4741) were incubated with radioactive acetate during a 3 h pulse period at 30°C. Following the pulse, nonsaponifiable lipids were extracted and separated on TLC plates along with authentic standards of squalene, oxidosqualene, dioxidosqualene, ketosteroid 1 (a mixture of 4-methylzymosterone and 4-methylfecosterone), ketosteroid 2 (a mixture of zymosterone and episterone, with the same Rf of dioxidosqualene), lanosterol and ergosterol (as a reference for 4-desmethylsterols). In wild type strains, no substantial accumulation of ketosteroids 1 and 2, which are direct substrates of Erg27p occurred in rho° conditions (Table 1), suggesting that, when Erg27p is relocalised in ER, the enzymatic activity is still present; this is confirmed by the fact that the *Δdga1/Δlro1/Δare1/Δare2* quadruple mutant, lacking LDs, still retains ergosterol production [44].

The observed general increase of % incorporation of all precursors of ergosterol, tested in rho° condition, suggests, although does not prove, a decrease in the kinetics of ergosterol biosynthesis.

3.5 The Retrograde pathway controls the *ERG27* expression in rho° cells

The block of the mitochondrial respiratory chain by antimycin A induces the activation of the Retrograde Pathway [49, 50], responsible for the modulation of nuclear transcription following a mitochondrial dysfunction. To verify if there was a modulation of *ERG27* gene transcription, we measured expression by real time RT-qPCR quantification of *ERG27* mRNA in cells with altered mitochondrial function, compared with the isogenic wild type strain. We analyzed also a strain unable to activate the Retrograde Pathway, Δ*rtg2* [51]. The RT-qPCR analysis showed that *ERG27* transcription was significantly induced in rho° cells (Figure 5) and this activation was dependent on the Retrograde Pathway because no modulation of *ERG27* mRNA was observed in Δ*rtg2* cells. As a control, we analyzed *ERG11* mRNA which showed no modulation in the absence of mitochondrial DNA or following treatment with antimycin A.

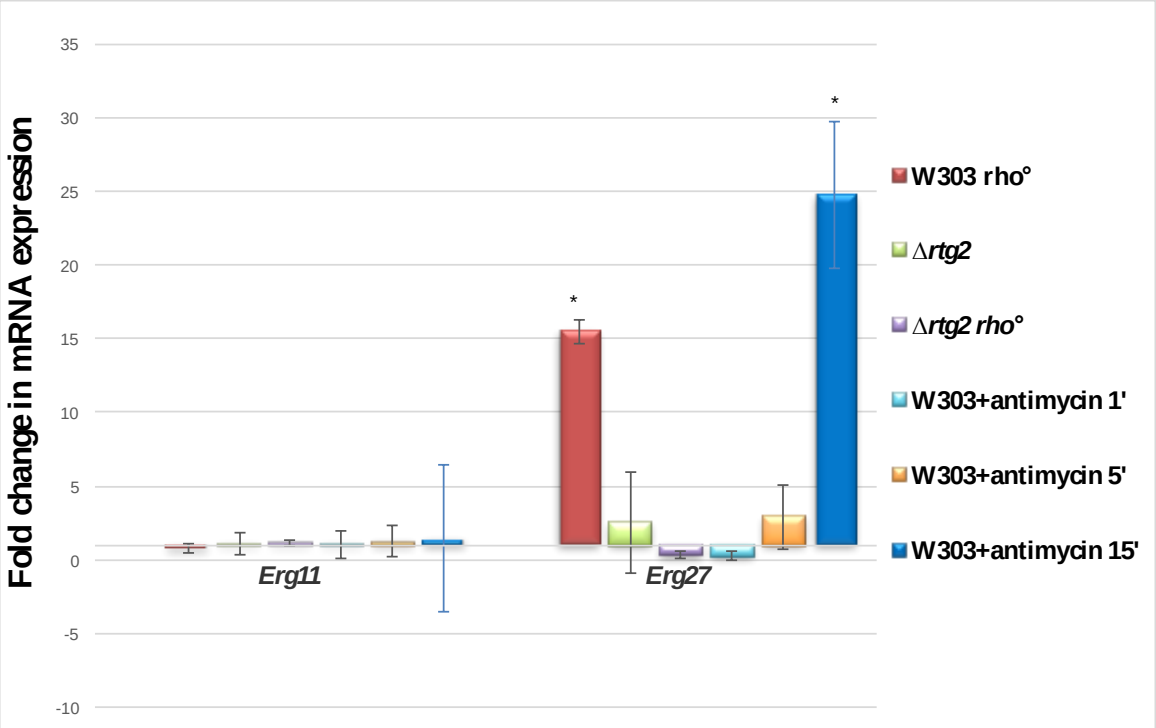

Figure 5. The Retrograde Pathway mediates the activation of *ERG27* transcription in the rho° strain. The *ERG27* transcription is induced in rho° strain and after antimycin treatment, while the level of *ERG11* remains unchanged. The histograms report the ratios between the mRNA of *ERG11* and *ERG27* in W303 rho°, in Δ*rtg2* and in W303 treated with antimycin. The wild type W303 untreated strain was set as 1. Data are the average of 4 independent experiments and standard deviation is indicated. The asterisks indicate significant modulations (*P<0.05) according to Student's T-test.

We then verified by Western Blot analysis the amount of Erg27p in rho° cells; compared with the wild type yeast cells, and we observed that the Erg27p is present in higher amount. The antimycin treatment also results in an increase of the Erg27p (Figure 6).

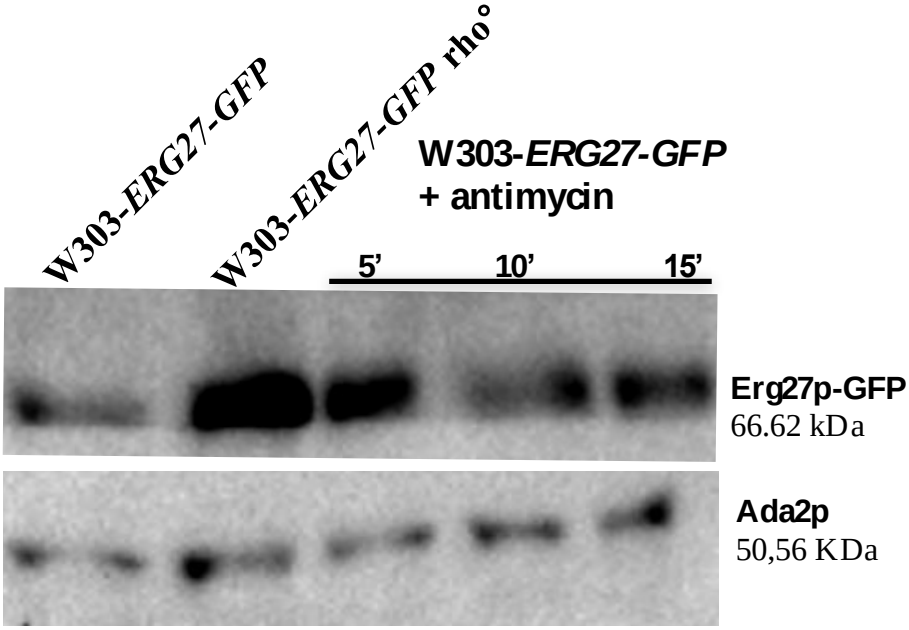

Figure 6. The Erg27p is in higher amount in rho° strain and in wild type strain after antimycin (10µg/ml) treatment. Western Blot analysis of W303 wild type strain, W303 rho° and W303 wild type strain treated with antimycin for 5, 10 and 15 minutes; the absence of mitochondrial DNA or antimycin treatment resulted in higher amount of Erg27p. Erg27p-GFP volume ratio bands with Image Lab 5.1 version software by Bio Rad: W303-*ERG27-GFP* 1,5934; W303-*ERG27-GFP* rho° 4,9201; W303-*ERG27-GFP* +5' antimycin 4,9482; W303-*ERG27-GFP* +10' antimycin 2,0313; W303-*ERG27-GFP* +15' antimycin 2,3670 of the respective *ADA2* bands.

Taken together these results showed that the lack of mitochondrial function stimulates the transcription and translation of *ERG27*, that this protein is localized in ER, where it is still active (its substrate doesn't accumulate), but in this condition, the ergosterol is synthesized in lower amount in the cells (see Discussion).

3.6 Ketoconazole, but not nystatin, induces loss of mitochondrial DNA

The results obtained pointed to an influence of the mitochondrial status on the biosynthetic ergosterol pathway, we then asked if, vice versa, a perturbation of the ergosterol biosynthetic pathway could affect the mitochondrial function. We used ketoconazole and nystatin, molecules with a different mechanism of action, to monitor the percentage of *petites* production in yeast (i.e. yeast cells unable to growth on respiratory substrate like glycerol, as the only carbon source). Ketoconazole, specifically inhibits the lanosterol 14-alpha demethylase enzyme (Erg11p); nystatin binds to ergosterol in the fungal membrane and it was chosen as a control because it doesn't affect the ergosterol biosynthesis pathway. Figure 7 shows the percentage

of *petites* production in wild type cells treated with increasing doses of ketoconazole and nystatin, followed for 24, 48 and 72 hours (Figure 7A and B, respectively). Ketoconazole significantly induces *petites* production at the concentration of 50µg/ml. These *petites* were rho° cells, i.e. devoid of mitochondrial DNA, as it was assessed by DAPI staining (Figure 7C). On the contrary, nystatin, at the concentration of 1µg/ml, resulted in a *petites* production of 53,38%, 30,97% and 16,33%, at 24 hours, 48 and 72 hours, respectively (Figure 7B), (see Discussion). Vitality of the strains presented in Figure 7 is reported in Supplemental Figure 2. These results suggest that a specific block of the ergosterol biosynthetic pathway induces a loss of mitochondrial DNA.

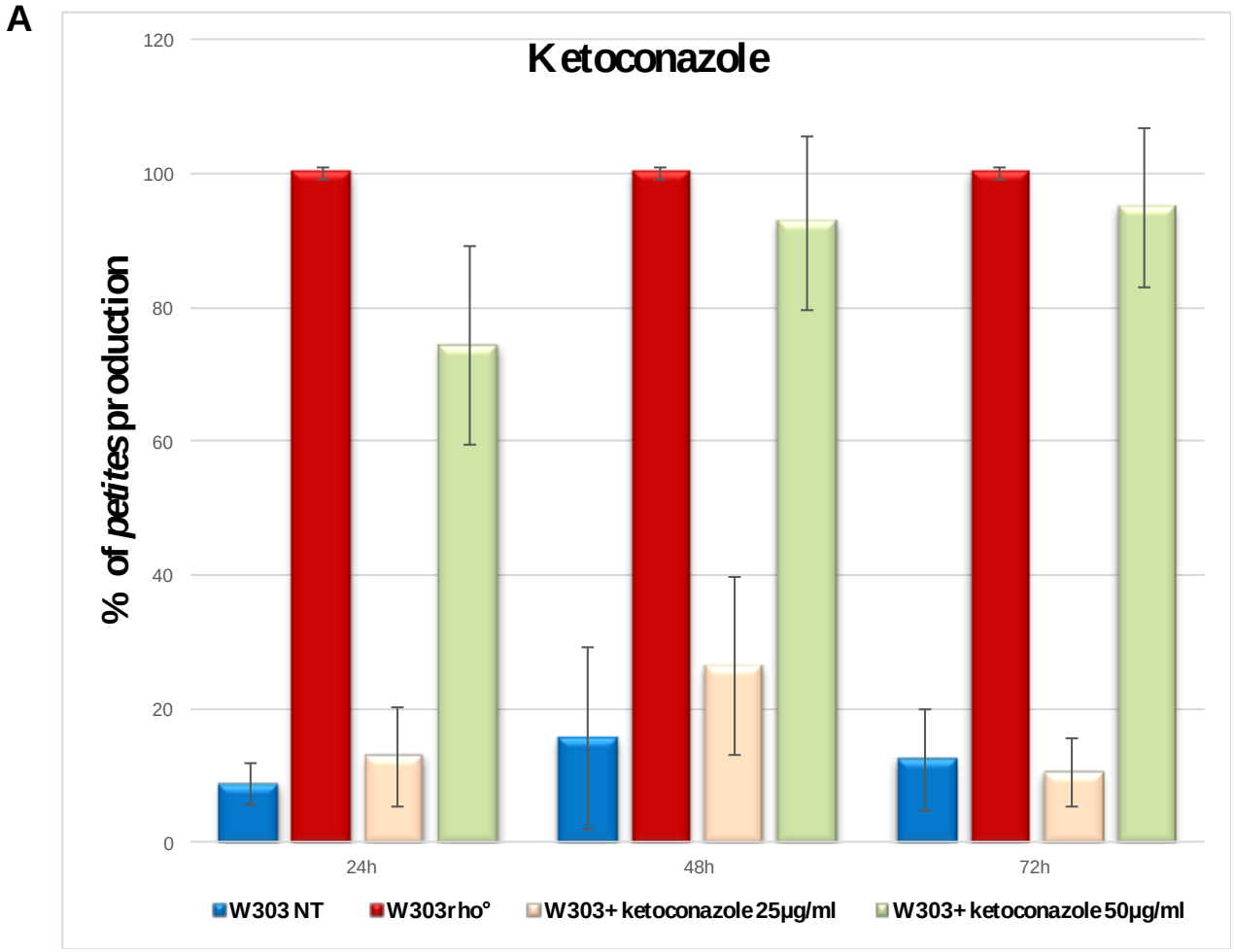

B

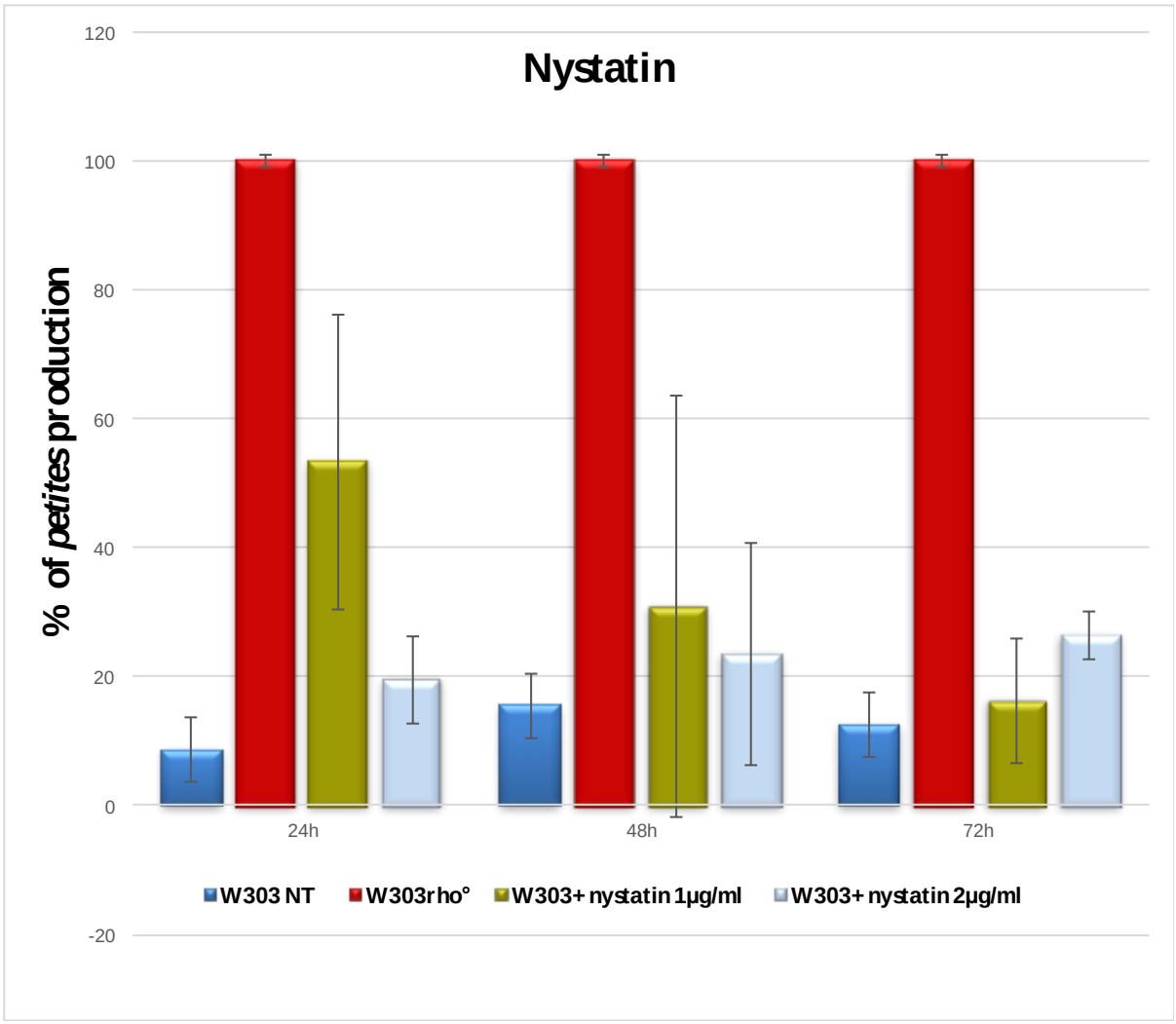

C

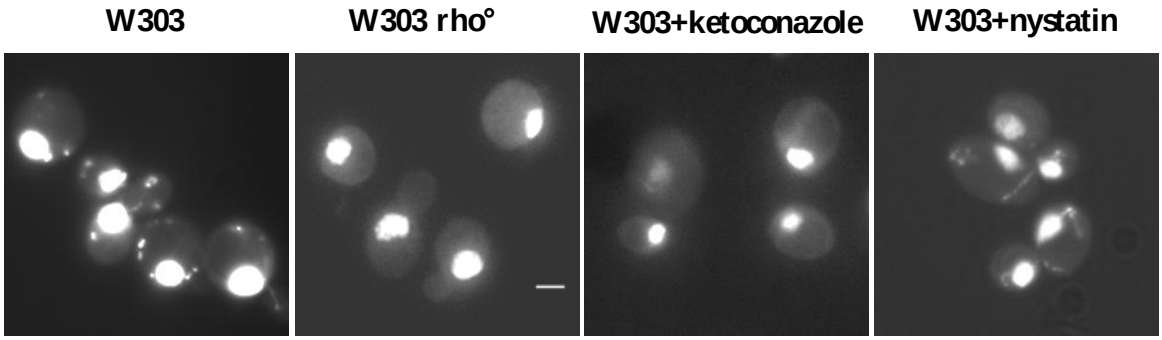

Figure 7. Percentage of *petites* production after treatment with nystatin and ketoconazole. A: ketoconazole treatment, which block ergosterol synthesis, induced a high rate of *petites* phenotype, due to the loss of mitochondrial DNA at the concentration of 50µg/ml. B: nystatin, which block ergosterol inserted in the plasma membrane, didn't show a significant alteration of mitochondrial DNA maintenance at the concentrations active in yeast. C: DAPI staining of cells presented in Figure A and B; wild type W303, W303 rho° and wild

type W303 treated with 50µg/ml of ketoconazole or 2µg/ml of nystatin (at 72 hours) are presented. Bar: 0.2µm. The magnification is the same in each picture.

3.7 Ergosterol suppresses the rho° production of Δ*erg27* strain

If the reduction or a block of the ergosterol biosynthetic pathway induces loss of mitochondrial DNA, we reasoned that also the deletion of *ERG27* should induce a *petites* phenotype and that the addition of ergosterol should suppress this phenotype. In *S. cerevisiae*, the *ERG27* is essential since its absence causes a complete block of ergosterol synthesis, but the Δ*erg27* strain associated with *upc2-1* mutation is able to grow in a medium supplemented with the minimal requirement of 0.02mg/ml of ergosterol. Upc2p is a general regulator of the expression of *ERG* genes [52-54] and the *upc2-1* mutation also increases the potency of the activation domain [55]. Since we cannot exclude an involvement of *upc2-1* mutation in the Δ*erg27* phenotypes, as a control, we also measured the percentage of *petites* in a Δ*erg27* strain transformed with the *ERG27* wild type gene (strain called Δ*erg27*+pST10(*ERG27*)). We cultured the Δ*erg27* strain in YPD medium supplemented with 0.02 and 0.5mg/ml of ergosterol and we counted the *petites* production after 24 and 48 hours of growth. Figure 8A shows that after 24 hours, the Δ*erg27* strain produced 45.01% of *petites*, compared with 2.86% of *petites* in the W303 wild type strain. After 48 hours, i.e. stationary phase, in the mutant supplemented with 0.02mg/ml ergosterol, the *petites* percentage raised to 80.76%, while the presence of 0.5mg/ml of ergosterol suppressed the *petites* production in the Δ*erg27* (20.32% of *petites* production), stabilizing the mitochondrial DNA. The Δ*erg27*+pST10(*ERG27)* doesn't show a *petites* phenotype, demonstrating that *upc2-1* mutation is not involved in the Δ*erg27 petites* phenotype.

These experiments showed that the absence of the ergosterol synthesis results in loss of mitochondrial DNA and that the external addition of ergosterol in higher amount (0.5mg/ml) than the minimal requirement (0.02mg/ml) to grow, is sufficient to maintain/stabilize the mitochondrial DNA. Figure 8B shows that the 0.5mg/ml of ergosterol in YPD medium suppressed the *petites* production in Δ*erg27* and that ergosterol is also able to suppress formation of *petites* production in Δ*mdm34* strain.

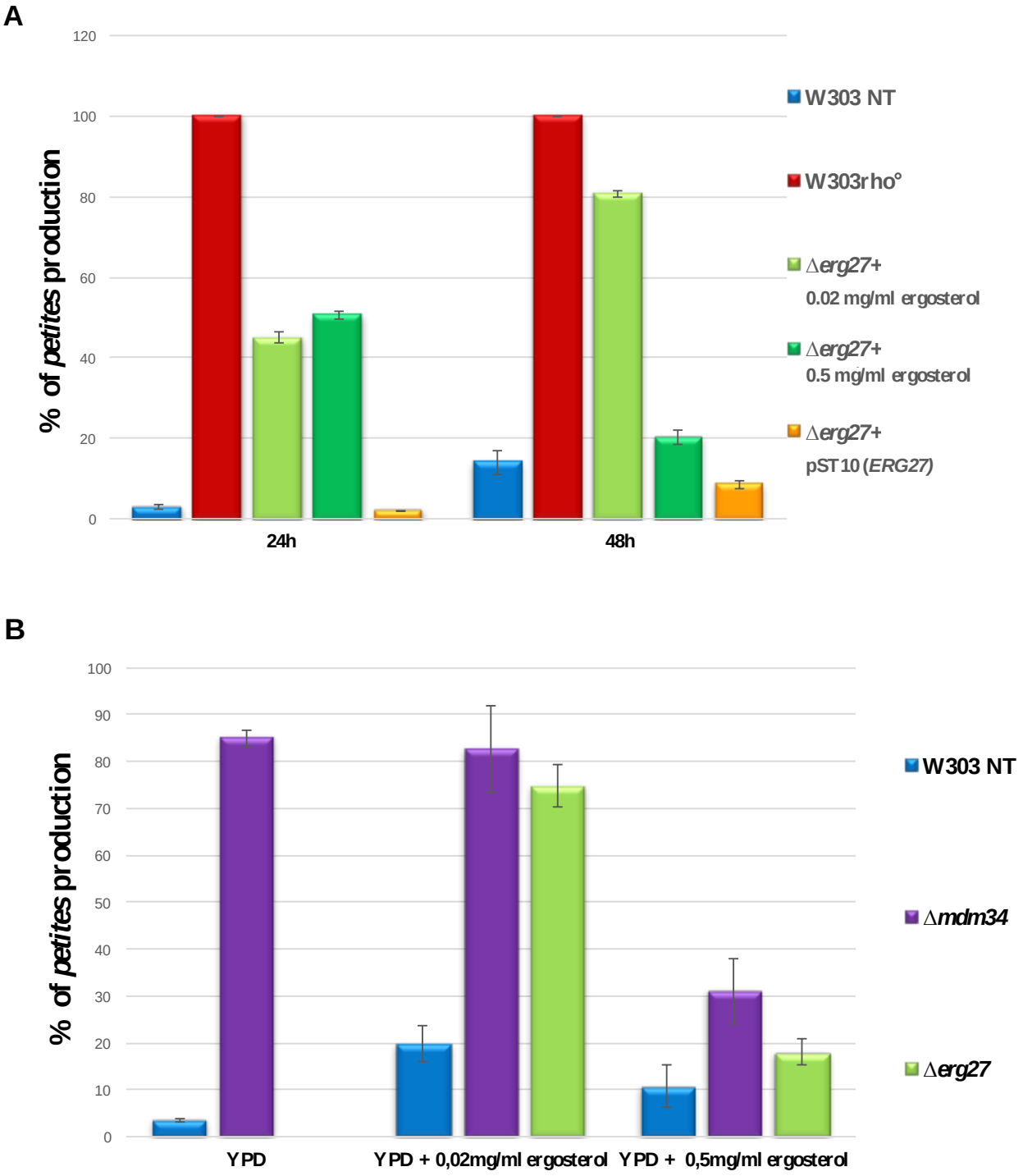

Figure 8. Ergosterol is essential for mitochondrial DNA maintenance. A: 0.02mg/ml of ergosterol are sufficient to promote Δ*erg27* growth but not to maintain mitochondrial DNA, while 0.5mg/ml of ergosterol in the

medium suppresses the percentage of *petites* production of Δ*erg27* strain. In presence of ergosterol in the medium, the Δ*erg27* strain shows 45.01% and 50.48% of *petites* at 24 hours in YPD medium supplemented with 0.02 or 0.5mg/ml of ergosterol, respectively. At 48 hours, while with 0.02mg/ml of ergosterol, the minimal concentration required for growth, the Δ*erg27* strain accumulates *petites* (80.76%), at the concentration of 0.5mg/ml ergosterol stabilizes the mtDNA (20.33% of *petites*). The Δ*erg27*+pST10(*ERG27*), containing the *upc2-1* mutation in a wild type *ERG27* genetic context, doesn't show a *petites* phenotype. B: Ergosterol also suppresses the *petites* production of Δ*mdm34* cells (from 85% to 31%). In YPD, the histogram corresponding to Δ*erg27* is not present because this strain doesn't grow without ergosterol. Data are the average of 5 independent experiments and standard deviation is indicated.

3.8 Mitochondrial morphology in rho° cells

The intimate connection between mitochondrial morphology and mitochondrial DNA maintenance has been deeply investigated [56], so we finally visualized the mitochondrial morphology of the Δ*erg27* strain transforming the cells with the pVT100UGFP plasmid, containing the mitochondria-targeted *GFP* (mitoGFP) gene [31]. Indeed, an altered mitochondrial phenotype was already observed for other genes of the ergosterol biosynthetic pathway using a regulatable promoter [29]. Figure 9A shows that yeast cells devoid of mitochondrial DNA (W303 rho°) contained disorganized mitochondria in YPD medium. The lack of the *ERG27* also resulted in an aberrant mitochondrial morphology: mitochondria are clearly fragmented and round similar to that of the cells without the ERMES complex (Δ*mdm34* cells). In the Δ*erg27* strain, the presence of the minimal concentration of ergosterol, (0.02mg/ml) required for growth, was not able to suppress the aberrant mitochondrial morphology; indeed, low concentration of ergosterol (0.02mg/ml) also didn't suppress the loss of mitochondrial DNA (Figure 8). We then looked at the mitochondrial morphology at the same conditions in which mitochondrial DNA is maintained in Δ*erg27* strain, i.e. YPD medium supplemented with 0.5mg/ml; in this growth condition, we observed a correct elongated mitochondrial morphology (Figure 9A) and, of note, this was observed also for the W303 rho° and Δ*mdm34* cells. Figure 9B shows the percentage of aberrant round mitochondrial morphology in exponential phase with different ergosterol concentrations. Taken together these results demonstrated the essential function of ergosterol in maintaining a correct mitochondrial morphology in yeast cells.

A

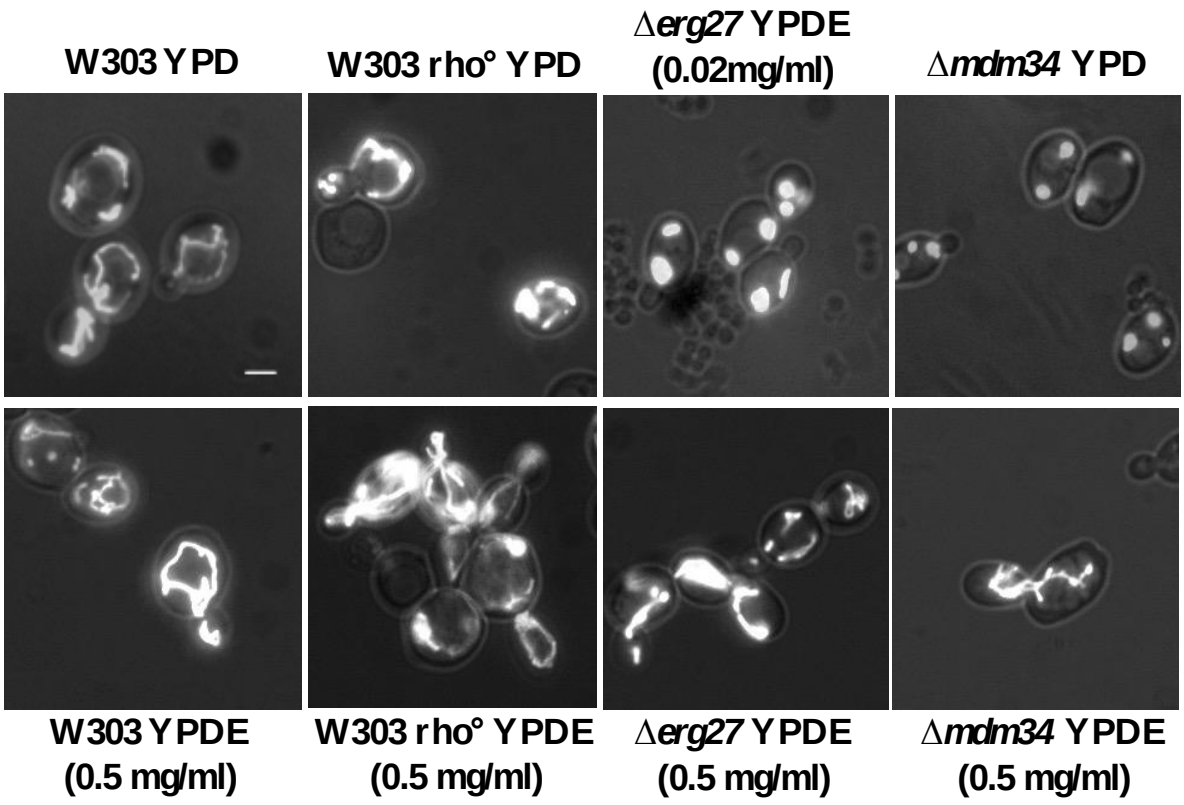
W303 YPD
W303 rho° YPD
Δerg27 YPDE (0.02mg/ml)
Δmdm34 YPD
W303 YPDE (0.5 mg/ml)
W303 rho° YPDE (0.5 mg/ml)
Δerg27 YPDE (0.5 mg/ml)
Δmdm34 YPDE (0.5 mg/ml)

B

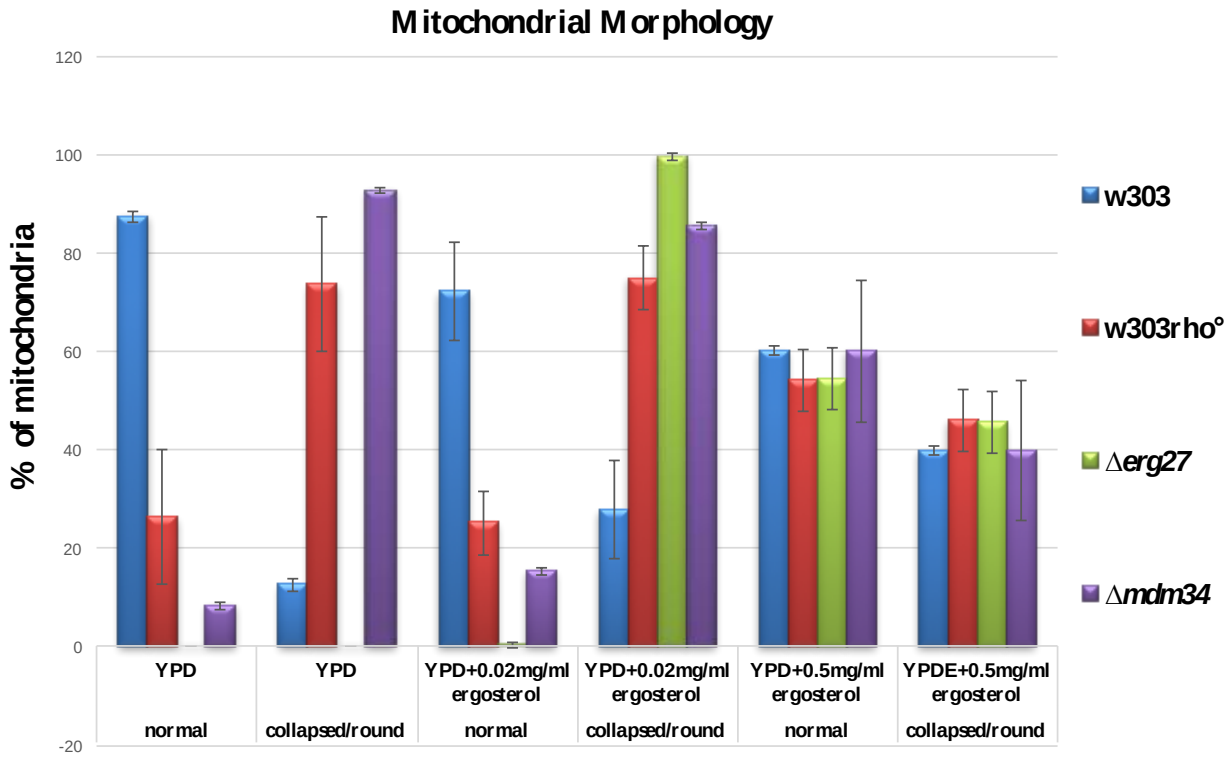
Mitochondrial Morphology
% of mitochondria
120
100
80
60
40
20
0
-20
YPD normal
YPD collapsed/round
YPD+0.02mg/ml ergosterol normal
YPD+0.02mg/ml ergosterol collapsed/round
YPD+0.5mg/ml ergosterol normal
YPDE+0.5mg/ml ergosterol collapsed/round
w303
w303rho°
Δerg27
Δmdm34

Figure 9. Ergosterol is essential for the maintenance of tubular mitochondrial morphology. A: mitochondrial morphology visualized with mito-GFP. The W303 wild type strain shows normal branched tubular mitochondria, while the rho° strain contains disorganized mitochondria. Δ*erg27* and Δ*mdm34* share the same mitochondrial phenotype, round collapsed mitochondria, this phenotype is suppressed by the addition of ergosterol in YPD medium. Bar: 2µm. The magnification is the same in each picture. B: Percentage of aberrant/round mitochondrial morphology of the strains described in A. The tubular and collapsed mitochondria were counted from pictures taken to produce Figure 9A; the histogram was obtained from the average of 3 distinct biological experiments, for each experiment mitochondrial morphology phenotypes were counted from 100 cells. Δ*erg27* strain shows 100% of collapsed round mitochondria when grow in YPD+ 0.02mg/ml of ergosterol, the minimal concentration required for growth. In YPD, without ergosterol addition, Δ*erg27* doesn't grow. When Δ*erg27* is supplemented with 0.5mg/ml of ergosterol, the % of cells with aberrant mitochondria drops to 67.52%. 0.5mg/ml of ergosterol suppresses also the mitochondrial morphology defect of the wild type rho° (from 83.40% to 41.50%) and Δ*mdm34* cells (from 92.18% to 62.29%).

4. Discussion

In yeast, ergosterol function in mitochondrial biogenesis has not been extensively studied, nevertheless its presence in higher amount in the IMM compared with the OMM should has a biological significance [9, 10, 12]. Previous observations suggest an involvement of the ERMES complex in ergosterol import since the absence of ERMES proteins altered the level of ergosterol in the cells [27]. Unfortunately, the balance between different class of lipids is highly regulated, rendering difficult to define if other complexes or proteins are involved in ergosterol import into the mitochondria.

Here, we showed that there is an interplay between the mitochondrial function and the ergosterol biosynthetic pathway, a cross talk resulting in a modulation of ergosterol content in cells with impaired mitochondrial function but also an induced loss of mitochondrial DNA and an altered mitochondrial morphology when the ergosterol biosynthetic pathway is blocked.

4.1 Mitochondrial dysfunction regulates ergosterol production

To demonstrate that Erg27p could be a "sensor" of mitochondrial dysfunction, we investigated two conditions in which the respiration is impaired: a) in a rho° context, i.e. cell lacking mtDNA and b) with a block of respiratory chain with antimycin A.

a) We found that in rho° cells the Retrograde Pathway activates the transcription of *ERG27*, that the new synthesized enzyme is found in ER and not in LDs as in wild type cells, and this localization results in an al-

teration of ergosterol levels in the cells. At our knowledge, this is the first observation that the Retrograde Pathway regulates the *ERG27*. We have not further investigated the transcription of other *ERG* genes in absence of mitochondrial function at this stage, except for *ERG11* chosen because its product is not localized in LDs. Indeed, *ERG11* showed no modulation in the absence of mitochondrial DNA or following treatment with antimycin A, neither in the wild type, nor in the *Δrtg2* strain, but this issue deserves more interest in the future. In rho° cells, the ergosterol content is lower as compared with the wild type strain. Our experiments demonstrate that the lower amount of ergosterol content in absence of Mdm34p (an ERMES complex subunit) is primarily due to mtDNA absence/lack of respiration and not to the impaired ERMES function in transporting this sterol into the mitochondria. Indeed, the ergosterol content in strains deleted for ERMES complex was previously investigated, but not in a strain deleted for *MDM34* [27].

b) The block of respiratory chain with antimycin A in wild type cells promoted a rapid migration of the preexisting Erg27p from LDs to ER. The observation that, if the respiratory chain is blocked by antimycin A, Erg27p is rapidly relocalised in ER from LDs, also indicates that the ER localization observed in rho° cells is not an artifact. Moreover, this is not the first described case of relocalization of an enzyme of the ergosterol biosynthetic pathway: Erg1p, with a dual localisation in the ER and LDs, was found to be redistributed from LDs to ER in low iron condition in the cells [57]. Moreover, the rapid movement of the Erg27p from LDs to ER in presence of antimycin A, in a few minutes, suggested the persistence of an intimate contact between these two organelles, supporting the hypothesis that the at least a subset of LDs remain physically connected with the ER [51, 56-62].

This part of our results suggests that, following the absence of respiration (caused by the lack of mtDNA or antimycin A treatment), Erg27p relocalizes in ER and that the newly synthesized Erg27p remains in ER and it is not targeted to LDs, resulting in a negative modulation of ergosterol production. It's worth noting that the ER and plasma membrane are tethered for at least 40% of the plasma membrane [63], raising the question if the presence of Erg27p in the cortical ER could facilitate and supply the ergosterol in plasma membrane in a condition (mitochondrial dysfunction) in which the ergosterol availability is low. Future experiments will address the point of how the movement of Erg27p enzyme selectively results in low ergosterol content in the cells. Concerning the movement of Erg27p, it is known that, in yeast, the Erg27p belongs to the C-4 demethylase protein complex which includes, besides Erg27p, the enzymes Erg25p (C-4 methyl oxi-

dase), Erg26p (C-4 decarboxylase, C-3 dehydrogenase), and the scaffold protein Erg28p [64], a key protein in the yeast sterol biosynthetic enzyme complex [65]. The Erg25-26-27-28p complex formation, however, does not appear an absolute requirement to/for Erg27p activity, as the enzyme can maintain its functionality as a free protein (O.B.S. and G.B., manuscript in preparation). This implies that the protein can move freely in cytoplasmic compartments without alter its function. Nevertheless, additional experiments will be needed to identify the signal which promotes the selective localization of Erg27p in ER, since Erg6p and Erg7p, both localized in LDs in a wild type strain, are not relocalized in ER in presence of mitochondrial dysfunction. It will be interesting to verify if an imbalance of NADP+, the Erg27p cofactor, could be implicated in the signaling or if protein modifications such as ubiquitination or phosphorylation are involved in Erg27p regulation.

Alternatively, the ergosterol content itself could be the signal for Erg27p translocation, since at least two other examples were published: the first example is the deletion of the *SPF1* gene, which causes a mistargeting of the tail-anchored mitochondrial proteins in the ER instead of in the outer mitochondrial membrane. This is due exclusively to low ergosterol content in the cells, suggesting that lipid composition between organelle membranes are sufficient to determine membrane integration specificity [66]; the second example is that, in human cells, lowering cholesterol or inhibiting de novo synthesis of ceramides at the ER causes translocation of Sig-1R receptor from the mitochondria-associated ER membranes (MAMs) to ER cisternae [67, 68].

Our results and recent literature point to the concept that some lipid enzymes dynamically concentrate in functionally defined ER regions and that can be relocalized following lipid needs [69]; an example is the triacylglycerol biosynthetic pathway which relocalize from ER to growing LDs [70].

4.2 Block of ergosterol biosynthetic pathway causes the loss of mtDNA

We investigated the mitochondrial DNA stability in two conditions in which the ergosterol biosynthetic pathway is impaired: a) specific block of ergosterol production with ketoconazole and b) a deletion of *ERG27* gene.

a) Ketoconazole is an antimycotic which specifically block the Erg11p function; at the concentration of 50µg/ml, after 72 hours of treatment, the percentage of *petites* production was 94.86% and these *petites* were rho° cells, i.e. yeast cells devoid of mtDNA. As a control, we treated cells with nystatin: this com-

pound binds ergosterol in the plasma membrane, promoting pore formation and it doesn't act directly on the ergosterol biosynthetic pathway; nystatin, at the concentration of 1μg/ml, resulted in a *petites* production of 53,38%, 30,97% and 16,33%, at 24 hours, 48 and 72 hours, respectively. The *petites* production in exponential phase (24 hours) could be explained as an indirect effect of nystatin: binding to ergosterol and altering the cellular membrane permeability, nystatin causes a potassium ion leakage [71]. This could indirectly perturb the mitochondrial K+ homeostasis [72], which has been described to alter mitochondrial respiration in mammalian cells [73]. In yeast, alteration of mitochondrial ion homeostasis could result in a limited *petites* production, especially in exponential phase, when cells are in active duplication. Of note, the vitality is always comparable to wild type at 24, 48 and 72 hours of growth (supplementary figure 2). Altogether, these results showed the essential and specific function of ergosterol in mtDNA maintenance.

b) Deletion of *ERG27*. The Δ*erg27* strain showed high *petites* production and ergosterol supply in the medium suppressed the loss of mtDNA. The enzymes of the ergosterol biosynthetic pathway, including the Erg 25-26-27p complex, are essential for growing in a non-supplemented medium, (see Figure 1) but yeast cells can growth when ergosterol is added to the medium in presence of the *upc2-1* mutation, because this allele allows for aerobic sterol uptake [30, 74-76]. We verified the minimal concentration (0.02mg/ml) necessary for cell survival in a strain lacking *ERG27* and we measured *petites* production in this condition: after 48 hours, 80.76% of cells were *petites* lacking mtDNA, but with the concentration of 0.5mg/ml of ergosterol in the medium, the same strain showed 20.32% of rho° cells, indicating that the supplementation of ergosterol, alone, could suppress the *petites* production phenotype. These results demonstrated, in a second independent way, the essential function of ergosterol in maintaining mtDNA.

An emerging mechanism to distribute mtDNA throughout the mitochondrial network is suggested by the proximity between mtDNA nucleoids and the sites of mitochondrial fission events observed both in budding yeast and mammalian cells (70–80% of division events occur near nucleoids) [77-79]. So, despite the proteins involved in ER-mitochondria tether are not conserved in evolution, these contact sites are essential for coupling the mitochondrial DNA replication and mitochondrial division, both in yeast and human cells [78, 80-83].

Indeed, cholesterol was demonstrated to be essential for human mitochondrial DNA maintenance [84]. The attachment of mitochondrial DNA to the IMM is related to lipid raft, membrane microdomains enriched in cholesterol and sphingolipids [85]. Although lipid rafts were initially thought to reside solely in the plasma membrane [86], increasing evidence suggests the presence of raft-like regions in internal organelles and in proteomic analysis of lipid raft enriched membrane, performed in human cells, also mitochondrial proteins were selected [87]. The structural determinants of proteins which perform their function in lipid raft has also been analyzed [88]; new methods and innovative techniques will permit to study these lipid rafts in the future [89].

4.3 Mitochondrial morphology in rho° cells

Previous studies reported that mutations or lower transcription of ergosterol genes resulted in abnormal mitochondrial morphology: instead of tubular structures, mitochondrial are collapsed and/or fragmented, suggesting the need of correct ergosterol level for maintaining the wild type tubular mitochondrial morphology [29]. We demonstrated that in the Δ*erg27* strain the mitochondrial morphology is similar to that of the Δ*mdm34* strain, in which mitochondria have a round, collapsed shape. The Δ*erg27* severe mitochondrial morphology phenotype is suppressed by adding ergosterol in the medium, revealing the essential function of ergosterol in maintaining the mitochondrial shape, in addition to mitochondrial DNA maintenance. Moreover, also the partial suppression of the Δ*mdm34* mitochondrial phenotype by ergosterol underlines the fundamental function of the ERMES complex in mitochondrial lipid homeostasis [27]. The wild type rho° cells, which contain less ergosterol, show aberrant mitochondrial morphology, again indicating the relation between the lack of mitochondrial DNA, which results in the absence of respiration and oxidative phosphorylation, and mitochondrial shape [82].

In conclusion, we have discovered an interplay between mitochondrial physiology and ergosterol production. The involvement of ergosterol in maintaining mitochondrial morphology and mitochondrial DNA is of extreme biological significance also because the fragmentation of mitochondrial structure and instability of mtDNA are strictly related to human diseases and apoptosis [90-93].

5. **Acknowledgements**

We thank Agnes Delahodde and Michela Esposito for providing the *Erg6-GFP* strain and Sergio Giannattasio for a very helpful discussion and for providing the Δ*rtg2* strain. T.R. thanks Laura Frontali for constant support on mitochondrial research and for sharing the invaluable experience on this field. This research was supported by the University of Torino [Fondo di Ricerca Locale (ex 60 %) 2015 and 2016] and Ateneo 2016 Sapienza RP116154AA336D5B and RP116154BE52D30E and MAECI PGR00746. A. C. was supported by Associazione Gian Franco Lupo ‘‘Un sorriso alla vita’’ Onlus.

6. Author contributions statement

A.C. performed the experiments; A.M. performed the mass spectrometry analysis and S.O.B. and G.B. analysed the *Erg27* precursors. M.M.B. and R.N. discussed and supervised the experiments and revised the text. T.R. conceived the study, performed the genetic and cell biology experiments and wrote the paper.

7. References

[1] G. Daum, N. D. Lees, M. Bard & R. Dickson, Biochemistry, cell biology and molecular biology of lipids of Saccharomyces cerevisiae, Yeast, 14 (1998), pp. 1471-1510.

[2] E. Stüven, A. Porat, F. Shimron, E. Fass, D. Kaloyanova, B. Brügger, ... & J. B. Helms, Intra-Golgi protein transport depends on a cholesterol balance in the lipid membrane, Journal of Biological Chemistry, 278 (2003), pp. 53112-53122.

[3] F. R. Maxfield & I. Tabas, Role of cholesterol and lipid organization in disease, Nature, 438 (2005), pp. 612.

[4] A. Aufschnaiter, V. Kohler, J. Diessl, C. Peselj, D. Carmona-Gutierrez, W. Keller, & S. Büttner, Mitochondrial lipids in neurodegeneration, Cell and Tissue Research, 367 (2017), pp. 125-140.

[5] M. Fryberg, A. C. Oehlschlager, & A. M. Unrau, Biosynthesis of ergosterol in yeast. Evidence for multiple pathways, Journal of the American Chemical Society, 95 (1973), pp. 5747-5757.

[6] F. Karst, & F. Lacroute, Ergosterol biosynthesis in Saccharomyces cerevisiae, Molecular and General Genetics MGG, 154 (1977), pp. 269-277.

[7] P. J. Espenshade & A. L. Hughes, Regulation of sterol synthesis in eukaryotes, Annual review of genetics, 41 (2007), pp. 401-427.

[8] A. H. Kachroo, J. M. Laurent, C. M. Yellman, A. G. Meyer, C. O. Wilke, & E. M. Marcotte, Systematic humanization of yeast genes reveals conserved functions and genetic modularity, Science, 348 (2015), pp. 921-925.

[9] E. Zinser, C. D. Sperka-Gottlieb, E. V. Fasch, S. D. Kohlwein, F. R. I. T. Z. Paltauf, & G. U. N. T. H. E. R. Daum, Phospholipid synthesis and lipid composition of subcellular membranes in the unicellular eukaryote Saccharomyces cerevisiae, Journal of bacteriology, 173 (1991), pp. 2026-2034.

[10] E. Zinser, F. Paltauf, & G. Daum, Sterol composition of yeast organelle membranes and subcellular distribution of enzymes involved in sterol metabolism, Journal of bacteriology, 175 (1993), pp. 2853-2858.

[11] M. Scharwey, T. Tatsuta, & T. Langer, Mitochondrial lipid transport at a glance, Journal of Cell Science 126 (2013), pp. 5317-5323.

[12] G. Tuller, & G. Daum. Import of sterols into mitochondria of the yeast Saccharomyces cerevisiae, FEBS letters, 372 (1995), pp. 29-32.

[13] A. A. Rowland, & G. K. Voeltz, Endoplasmic reticulum–mitochondria contacts: function of the junction, Nature reviews Molecular cell biology, 13 (2012), pp. 607-625.

[14] A. Lang, A. T. J. Peter, & B. Kornmann, ER–mitochondria contact sites in yeast: beyond the myths of ERMES, Current opinion in cell biology, 35 (2015), pp. 7-12.

[15] M. J. Phillips, & G. K. Voeltz, Structure and function of ER membrane contact sites with other organelles, Nature reviews Molecular cell biology, 17 (2016), pp. 69-82.

[16] C. Voss, S. Lahiri, B. P. Young, C. J. Loewen, & W. A. Prinz, ER-shaping proteins facilitate lipid exchange between the ER and mitochondria in S. cerevisiae, J Cell Sci, 125 (2012), pp. 4791-4799.

[17] J. P. Fernández-Murray, & C. R. McMaster, Lipid synthesis and membrane contact sites: a crossroads for cellular physiology, Journal of lipid research, 57 (2016), pp. 1789-1805.

[18] B. Kornmann, E. Currie, S. R. Collins, M. Schuldiner, J. Nunnari, J. S. Weissman, & P. Walter, An ER-mitochondria tethering complex revealed by a synthetic biology screen, Science, 325 (2009), pp. 477-481.

[19] B. Kornmann, & P. Walter, ERMES-mediated ER-mitochondria contacts: molecular hubs for the regulation of mitochondrial biology, J Cell Sci, 123 (2010), pp. 1389-1393.

[20] J. R. Friedman, L. L. Lackner, M. West, J. R. DiBenedetto, J. Nunnari, & G. K. Voeltz, ER tubules mark sites of mitochondrial division, Science, 334 (2011), pp. 358-362.

[21] G. Szabadkai, K. Bianchi, P. Várnai, D. De Stefani, M. R. Wieckowski, D. Cavagna, A. I. Nagy, T. Balla, and R. Rizzuto, Chaperone-mediated coupling of endoplasmic reticulum and mitochondrial Ca2+ channels, J. Cell Biol., 175 (2006), pp. 901–911.

[22] O. M. de Brito, and L. Scorrano, Mitofusin 2 tethers endoplasmic reticulum to mitochondria, Nature, 456 (2008), pp. 605–610.

[23] R. Iwasawa, A. L. Mahul-Mellier, C. Datler, E. Pazarentzos, and S. Grimm, Fis1 and Bap31 bridge the mitochondria-ER interface to establish a platform for apoptosis induction, EMBO J., 30 (2011), pp. 556–568.

[24] Y. Hirabayashi, S. K. Kwon, H. Paek, W. M. Pernice, M. A. Paul, J. Lee, ... & F. Polleux, ER-mitochondria tethering by PDZD8 regulates Ca2+ dynamics in mammalian neurons, Science, 358 (2017), pp. 623-630.

[25] C. Osman, D. R. Voelker, & T. Langer, Making heads or tails of phospholipids in mitochondria, The Journal of cell biology, 192 (2011), pp. 7-16.

[26] M. A. Frohman, Role of mitochondrial lipids in guiding fission and fusion, Journal of Molecular Medicine, 93 (2015), pp. 263-269.

[27] T. Tan, C. Özbalci, B. Brügger, D. Rapaport, & K. S. Dimmer, Mcp1 and Mcp2, two novel proteins involved in mitochondrial lipid homeostasis, J Cell Sci., 126 (2013), pp. 3563-3574.

[28] K. S. Dimmer, S. Fritz, F. Fuchs, M. Messerschmitt, N. Weinbach, W. Neupert, & B. Westermann, Genetic Basis of Mitochondrial Function and Morphology in Saccharomyces cerevisiae, Molecular biology of the cell, 13 (2002), pp. 847-853.

[29] K. Altmann, & B. Westermann, Role of essential genes in mitochondrial morphogenesis in Saccharomyces cerevisiae, Molecular biology of the cell, 16 (2005), pp. 5410-5417.

[30] S. Taramino et al., Divergent interactions involving the oxidosqualene cyclase and the steroid-3-ketoreductase in the sterol biosynthetic pathway of mammals and yeasts, Biochimica et Biophysica Acta, 1801 (2010), pp. 1232–1237.

[31] B. Westermann, & W. Neupert, Mitochondria-targeted green fluorescent proteins: convenient tools for the study of organelle biogenesis in Saccharomyces cerevisiae. Yeast, 16(15), (2000), pp. 421-1427.

[32] A. A. Andreasen, & T. J. B. Stier. Anaerobic nutrition of Saccharomyces cerevisiae. I. Ergosterol requirement for growth in a defined medium. Journal of Cellular and Comparative Physiology, 41(1), (1953), pp. 23-36.

[33] C. Verduyn, E. Postma, W. A. Scheffers, & J. P. van Dijken, Physiology of Saccharomyces Cerevisiae in anaerobic glucose-limited chemostat culturesx. Microbiology, 136(3), (1990), pp. 395-403.

[34] D. Ottaviano, A. Montanari, L. De Angelis, R. Santomartino, A. Visca, L. Brambilla, ... & M. M. Bianchi. Unsaturated fatty acids-dependent linkage between respiration and fermentation revealed

by deletion of hypoxic regulatory KlMGA2 gene in the facultative anaerobe-respiratory yeast Kluyveromyces lactis, FEMS yeast research, 15(5), (2015).

[35] P. Greenspan, E. P. Mayer, & S. D. Fowler, Nile red: a selective fluorescent stain for intracellular lipid droplets, The Journal of cell biology, 100 (1985), pp. 965-973.

[36] A. Cirigliano, A. Stirpe, S. Menta, M. Mori, D. Dell'Edera, E. Pick, ... & T. Rinaldi. Yeast as a tool to select inhibitors of the cullin deneddylating enzyme Csn5, Journal of enzyme inhibition and medicinal chemistry, 31(6), (2016), pp. 1632-1637.

[37] C. White & J. Zainasheff. Yeast: the practical guide to beer fermentation. Brewers Publications. (2010), pp. 252.

[38] J. Pu, C. W. Ha, S. Zhang, J. P. Jung, W. K. Huh, & P. Liu, Interactomic study on interaction between lipid droplets and mitochondria, Protein & cell, 2 (2011), pp. 487-496.

[39] K. Natter, P. Leitner, A. Faschinger, H. Wolinski, S. McCraith, S. Fields, & S. D. Kohlwein, The spatial organization of lipid synthesis in the yeast Saccharomyces cerevisiae derived from large scale green fluorescent protein tagging and high resolution microscopy, Molecular & Cellular Proteomics, 4 (2005), pp. 662-672.

[40] M. J. Youngman, A. E. A. Hobbs, S. M. Burgess, M. Srinivasan, & R. E. Jensen. Mmm2p, a mitochondrial outer membrane protein required for yeast mitochondrial shape and maintenance of mtDNA nucleoids, The Journal of cell biology, 164(5), (2004), pp. 677-688.

[41] M. van der Laan, M. Bohnert, N. Wiedemann, & N. Pfanner. Role of MINOS in mitochondrial membrane architecture and biogenesis, Trends in cell biology, 22(4), (2012), 185-192.

[42] A. Murley, L. L. Lackner, C. Osman, M. West, G. K. Voeltz, P. Walter, & J. Nunnari. ER-associated mitochondrial division links the distribution of mitochondria and mitochondrial DNA in yeast, Elife, 2, (2013), e00422.

[43] S. D. Kohlwein, M. Veenhuis, & I. J. van der Klei, Lipid droplets and peroxisomes: key players in cellular lipid homeostasis or a matter of fat—store'em up or burn'em down, Genetics, 193 (2013), pp. 1-50.

[44] D. Sorger, K. Athenstaedt, C. Hrastnik, & G. Daum, A yeast strain lacking lipid particles bears a defect in ergosterol formation, Journal of Biological Chemistry, 279 (2004), pp. 31190-31196.

[45] A. Montanari, C. De Luca, L. Frontali, & S. Francisci, Aminoacyl-tRNA synthetases are multivalent suppressors of defects due to human equivalent mutations in yeast mt tRNA genes, Biochimica et Biophysica Acta (BBA)-Molecular Cell Research, 180 (2010), pp. 1050-1057.

[46] C. Mo, P. Milla, K. Athenstaedt, R. Ott, G. Balliano, G. Daum, & M. Bard. In yeast sterol biosynthesis the 3-keto reductase protein (Erg27p) is required for oxidosqualene cyclase (Erg7p) activity, Biochimica et Biophysica Acta (BBA)-Molecular and Cell Biology of Lipids, 1633 (2003), pp. 68-74.

[47] S. Oliaro-Bosso, S. Taramino, F., Viola, S. Tagliapietra, G. Ermondi, G. Cravotto, & G. Balliano, Umbelliferone aminoalkyl derivatives as inhibitors of human oxidosqualene-lanosterol cyclase, Journal of enzyme inhibition and medicinal chemistry, 24 (2009), pp. 589-598.

[48] S. Taramino, M. Valachovic, S. Oliaro-Bosso, F. Viola, B. Teske, M. Bard, G. Balliano, Interactions of oxidosqualene cyclase (Erg7p) with 3-keto reductase (Erg27p) and other enzymes of sterol biosynthesis in yeast, Biochimica et Biophysica Acta, 1801 (2010), pp. 156–162).

[49] C. B. Epstein, J. A. Waddle, W. Hale, V. Davé, J. Thornton, T. L. Macatee, ... & R. A. Butow. Genome-wide responses to mitochondrial dysfunction, Molecular Biology of the Cell, 12 (2001), pp. 297-308.

[50] Z. Liu, & R. A. Butow, Mitochondrial retrograde signaling, Annu. Rev. Genet., 40 (2006), pp. 159-185.

[51] X. Liao, & R. A. Butow, RTG1 and RTG2: two yeast genes required for a novel path of communication from mitochondria to the nucleus, Cell., 72 (1993), pp. 61-71.

[52] Å. Vik, & J. Rine, Upc2p and Ecm22p, dual regulators of sterol biosynthesis in Saccharomyces cerevisiae. Molecular and Cellular Biology, 21(19), (2001), pp. 6395-6405.

[53] B. S. Davies, & J. Rine, A role for sterol levels in oxygen sensing in Saccharomyces cerevisiae. Genetics, (2006).

[54] I. M. Joshua, & T. Höfken, From lipid homeostasis to differentiation: old and new functions of the zinc cluster proteins Ecm22, Upc2, Sut1 and Sut2. International journal of molecular sciences, 18(4), (2017), pp. 772.

[55] B. S., Davies, H. S., Wang, & J. Rine, Dual activators of the sterol biosynthetic pathway of Saccharomyces cerevisiae: similar activation/regulatory domains but different response mechanisms. Molecular and cellular biology, 25(16), (2005), pp. 7375-7385.

[56] T. Hanekamp, M. K. Thorsness, I. Rebbapragada, E. M. Fisher, C. Seebart, M. R. Darland, ... & P. E. Thorsness, Maintenance of mitochondrial morphology is linked to maintenance of the mitochondrial genome in Saccharomyces cerevisiae, Genetics, 162 (2002), pp. 1147-1156.

[57] M. Shakoury-Elizeh, O. Protchenko, A. Berger, J. Cox, K. Gable, T. M. Dunn, ... & C. C. Philpott, Metabolic response to iron deficiency in Saccharomyces cerevisiae, Journal of Biological Chemistry, 285 (2010), pp. 14823-14833.

[58] N. Jacquier, V. Choudhary, M. Mari, A. Toulmay, F. Reggiori, & R. Schneiter, Lipid droplets are functionally connected to the endoplasmic reticulum in Saccharomyces cerevisiae, J Cell Sci, 124 (2011), pp. 2424-2437.

[59] T. C. Walther, & R. V. Farese Jr, Lipid droplets and cellular lipid metabolism, Annual review of biochemistry, 81 (2012), pp. 687-714.

[60] A. R. Thiam, & M. Beller, The why, when and how of lipid droplet diversity, J Cell Sci, 130 (2017), pp. 315-324.

[61] A. S. Joshi, H. Zhang, & W. A. Prinz, Organelle biogenesis in the endoplasmic reticulum, Nature Cell Biology, 19 (2017), pp. 876-882.

[62] A. M. Valm, S. Cohen, W. R. Legant, J. Melunis, U. Hershberg, E. Wait, ... & J. Lippincott-Schwartz, Applying systems-level spectral imaging and analysis to reveal the organelle interactome, Nature, 546 (2017), pp. 162-167.

[63] S. Muallem, W. Y. Chung, A. Jha, & M. Ahuja, Lipids at membrane contact sites: cell signaling and ion transport, EMBO reports, 18 (2017), pp. 1893-1904.

[64] D. Gachotte, J. Eckstein, R. Barbuch, T. Hughes, C. Roberts, & M. Bard, A novel gene conserved from yeast to humans is involved in sterol biosynthesis, Journal of lipid research, 42 (2001), pp. 150-154.

[65] C. Mo, & M. Bard Erg28p is a key protein in the yeast sterol biosynthetic enzyme complex, Journal of lipid research, 46 (2005), pp. 1991-1998.

[66] K. Krumpe, I. Frumkin, Y. Herzig, N. Rimon, C. Özbalci, B. Brügger, ... & M. Schuldiner, Ergosterol content specifies targeting of tail-anchored proteins to mitochondrial outer membranes, Molecular biology of the cell, 23 (2012), pp. 3927-3935.

[67] T. Hayashi, & M. Fujimoto, Detergent-resistant microdomains determine the localization of σ-1 receptors to the endoplasmic reticulum-mitochondria junction, Molecular pharmacology, 77 (2010), pp. 517-528.

[68] M. Fujimoto, T. Hayashi, & T. P. Su, The role of cholesterol in the association of endo-plasmic reticulum membranes with mitochondria, Biochemical and biophysical research communications, 417 (2012), pp. 635-639.

[69] J. Jacquemyn, A. Cascalho, & R. E. Goodchild, The ins and outs of endoplasmic reticulum-controlled lipid biosynthesis, EMBO reports, 18 (2017), pp. 1905-1921.

[70] F. Wilfling, H. Wang, J. T. Haas, N. Krahmer, T. J. Gould, A. Uchida, ... & X. Liu, Triacylglycerol synthesis enzymes mediate lipid droplet growth by relocalizing from the ER to lipid droplets, Developmental cell., 24 (2013), pp. 384-399.

[71] S. M. Hammond, P. A. Lambert, & B. N. Kliger, The mode of action of polyene antibiotics; induced potassium leakage in Candida albicans. Microbiology, 81(2), (1974), pp. 325-330.

[72] D. Malinska, S. R. Mirandola, & W. S. Kunz, Mitochondrial potassium channels and reactive oxygen species. FEBS letters, 584(10), (2010), pp. 2043-2048.

[73] A. Szewczyk, W. Jarmuszkiewicz, & W. S. Kunz, Mitochondrial potassium channels. IUBMB life, 61(2), (2009), pp. 134-143.

[74] T. L. Lewis, G. A. Keesler, G. P. Fenner, & L. W. Parks. Pleiotropic mutations in Saccharomyces cerevisiae affecting sterol uptake and metabolism, Yeast, 4(2), (1988), pp. 93-106.

[75] J. V. Layer, B. M. Barnes, R. Y. Yamasaki, Li. L. Barbuch, S. Taramino, ... & M. Bard, Characterization of a mutation that results in independence of oxidosqualene cyclase (Erg7) activity from the downstream 3-ketoreductase (Erg27) in the yeast ergosterol biosynthetic pathway. Biochimica et Biophysica Acta (BBA)-Molecular and Cell Biology of Lipids, 1831(2), (2013), pp. 361-369.

[76] L. J. Wilcox, D. A. Balderes, B. Wharton, A. H. Tinkelenberg, G. Rao, & S. L. Sturley, Transcriptional profiling identifies two members of the ATP-binding cassette transporter superfamily re-

quired for sterol uptake in yeast. Journal of Biological Chemistry, 277(36), (2002), pp. 32466-32472.

[77] V. Jayashankar, & S. M. Rafelski, Integrating mitochondrial organization and dynamics with cellular architecture, Current Opinion in Cell Biology, 26 (2014), pp. 34-40.

[78] A. Murley, L. L. Lackner, C. Osman, M. West, G. K. Voeltz, P. Walter, & J. Nunnari, ER-associated mitochondrial division links the distribution of mitochondria and mitochondrial DNA in yeast, Elife, 2 (2013) e00422.

[79] R. Ban-Ishihara, T. Ishihara, N. Sasaki, K. Mihara, & N. Ishihara, Dynamics of nucleoid structure regulated by mitochondrial fission contributes to cristae reformation and release of cytochrome c, Proceedings of the National Academy of Sciences, 110 (2013), pp. 11863-11868.

[80] S. C. Lewis, L. F. Uchiyama, & J. Nunnari, ER-mitochondria contacts couple mtDNA synthesis with mitochondrial division in human cells, Science, 353 (2016) aaf5549.

[81] L. Abelovska, Mitochondria as protean organelles: membrane processes that influence mitochondrial shape in yeast, Gen Physiol Biophys, 30 (2011), pp. S13–S24.

[82] J. R. Friedman, & J. Nunnari, Mitochondrial form and function, Nature, 505 (2014), pp. 335.

[83] A. Murley, & J. Nunnari, The emerging network of mitochondria-organelle contacts, Molecular cell., 61 (2016), pp. 648-653.

[84] J. M. Gerhold, Ş. Cansiz-Arda, M. Lõhmus, O. Engberg, A. Reyes, H. van Rennes, ... & J. N. Spelbrink, Human Mitochondrial DNA-Protein Complexes Attach to a Cholesterol-Rich Membrane Structure, Scientific reports, 5 (2015), pp. 15292-15292.

[85] E. Sezgin, I. Levental, S. Mayor, & C. Eggeling, The mystery of membrane organization: composition, regulation and roles of lipid rafts, Nature Reviews Molecular Cell Biology, 18 (2017), pp. 361–374.

[86] K. Simons, & E. Ikonen. Functional rafts in cell membranes, Nature, 387 (1997), pp. 569.

[87] C. N. Poston, E. Duong, Y. Cao, & C. R. Bazemore-Walker, Proteomic analysis of lipid raft-enriched membranes isolated from internal organelles, Biochemical and biophysical research communications, 415 (2011), pp. 355-360.

[88] J. H. Lorent, & I. Levental, Structural determinants of protein partitioning into ordered membrane domains and lipid rafts, Chemistry and physics of lipids, 192 (2015), pp. 23-32.

[89] M. Carquin, L. D'Auria, H. Pollet, E. R. Bongarzone, & D. Tyteca, Recent progress on lipid lateral heterogeneity in plasma membranes: From rafts to submicrometric domains, Progress in lipid research, 62 (2016), pp. 1-24.

[90] A. B. Knott, G. Perkins, R. Schwarzenbacher, & E. Bossy-Wetzel, Mitochondrial fragmentation in neurodegeneration, Nature reviews Neuroscience, 9 (2008), pp. 505.

[91] B. Westermann, Mitochondrial fusion and fission in cell life and death, Nature reviews Molecular cell biology, 11 (2010), pp. 872.

[92] S. L. Archer, Mitochondrial dynamics—mitochondrial fission and fusion in human diseases, New England Journal of Medicine, 369 (2013), pp. 2236-2251.

[93] T. Ferrante, et al, "4-Methylzymosterone and Other Intermediates of Sterol Biosynthesis from Yeast Mutants Engineered in the ERG27 Gene Encoding 3-Ketosteroid Reductase", 51.9 (2016), pp. 1103-1113.

& Yeast: the practical guide to beer fermentation. Brewers Publications.

Table 1. [^{14}C] acetate incorporation into the non-saponifiable lipid fraction of *S. cerevisiae* strains.

Strain	% total radioactivity incorporated					
	Squalene	Oxido squalene	Dioxido Squalene/ Ketosteroid 2 [b]	Ketosteroid 1 [a]	Lanosterol	4-desmethylsterols
BY4741	18.6	0.4	0.5	0.6	1.6	78.3
BY4741 rho°	21.2	1.6	4.9	4.1	6.2	62.0
W303	15.6	0.8	1.1	0.9	2.1	79.5
W303 rho°	27.9	1.1	3.3	1.9	2.1	63.7

[a] ketosteroid 1 is a mixture of 4-methylzymosterone and 4-methylfecosterone. [76]
[b] ketosteroid 2 is a mixture of zymosterone and episterone.[76]
Values are the means of three separate experiments, each one carried out in duplicate. The maximum deviations from the mean were less than 10%.

Supplemental Figures

Supplemental Figure 1. Erg7p-GFP is correctly localized in LDs in wild type and its corresponding rho° strain. Bar: 0.5µm. In both W303 and BY4741 context, the rho° cells show the Erg27p-GFP de-localization.

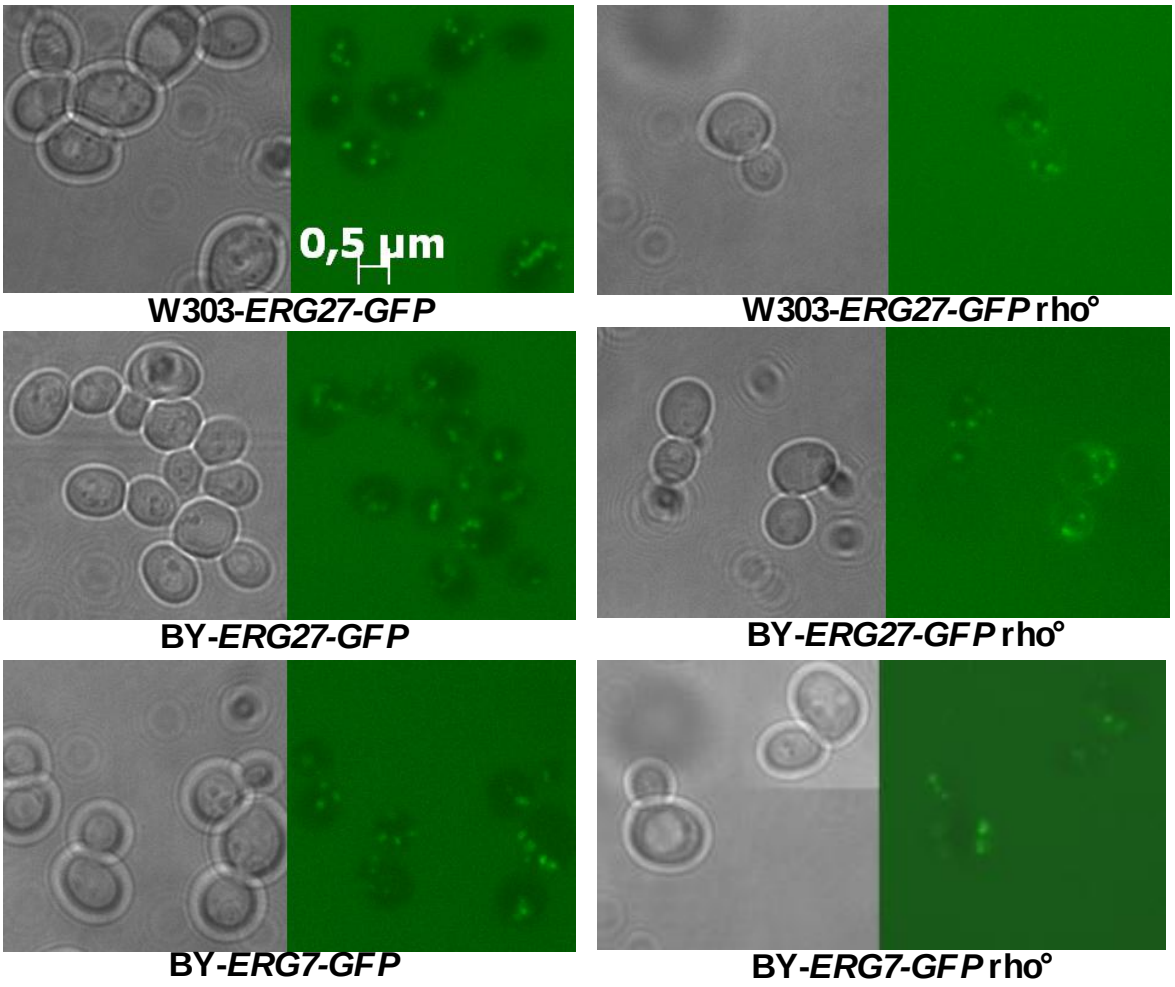

Supplemental Figure 2. Vitality of the strains presented in Figure 7A and 7B. Data are the average of 5 independent experiments and standard deviation is indicated.

The strains were inoculated in YPD rich medium and after 24 hours of treatment with nystatin and ketoconazole at different concentrations, cells were counted and 100 cells were plated on YPD plates; after growth, we counted 100 colonies, which correspond to 100% of vitality (24h). The same experiment was performed after 48, 72 and 96 hours, to obtain vitality data.